UNIVERSITY OF DEBRECEN
FACULTY OF ENGINEERING
DEPARTMENT OF
MECHANICAL ENGINEERING

INVESTIGATION OF TOOL WEAR PATTERN AND THEIR OPTIMIZATION IN SINGLE-POINT CUTTING TOOL

THESIS

Jean Pierre HITIMANA
Mechanical Engineering

Debrecen
2024

Table of Contents

Table of notations

V_B [mm]	wear land
K_T [mm]	Taper wear
F [N]	Force
V [m/s]	Velocity

1 Introduction

Cutting with high efficiency is a crucial aspect of ensuring sustainability in manufacturing. Tool wear is a vital problem in machining processes because it reduces the surface finish quality and makes the workpiece dimensions less predictable[1]. Tool wear leads to the roughening of the tool surface and the distortion of its ridges. It also increases the cutting force, residual stress, and temperature. Tool wear is a critical factor in the machining processes, as it can impact product quality and efficiency [2]. Despite the high level of automation in the machining industry, tool wear remains a challenge to automate the turning process fully. Tool wear is a common phenomenon that happens to cutting tools because of the result of thermal, chemical, and mechanical pressures during machining [3]. When cutting tools are used continuously during the chip generation, they gradually deteriorate. This can lead to increased cutting ability and further machining power, which lowers the surface quality to be machined [3].

For companies to improve their productivity, they must optimize all their production processes, including the cutting procedures. Industry uses extremely high cutting processes (high feed rates and cutting speeds) to achieve this. Mechanical stress, the tool temperature and the chip connection and surrounding the machining regime. This can lead to an excessive amount of wear on the tool or possibly cause the tool to fail before its expected lifespan. Thus, to maintain the increase in machining productivity, a realistic simulation of the cutting process must be created to determine the ideal cutting conditions for tool material, tool shape, and coating. In this research, I will investigate different wear patterns and their optimization in single-point cutting tools in four tasks that are: Overview the theoretical background on different tool wear patterns, Create a 3D model of the cutting tool deformation during machining, Carry out Finite Element Analysis for the tool patterns, Evaluation of the results and comparison with scientific research resources

2 Overview of the theoretical background on different tool wear patterns

2.1 Review of existing literature

Valery Marinov[4] The topic of tool wear and tool life in manufacturing technology involves the examination of three primary forms of tool wear: crater wear, flank wear, and corner wear. Crater wear is the depression on the face of the tool that affects how a tool cuts. Flank wear arises from the friction between the tool and the workpiece, exerting a notable influence on the cutting forces. Crater wear occurs on the tool's corner and can cause the ma\chined part to be the wrong size or shape.

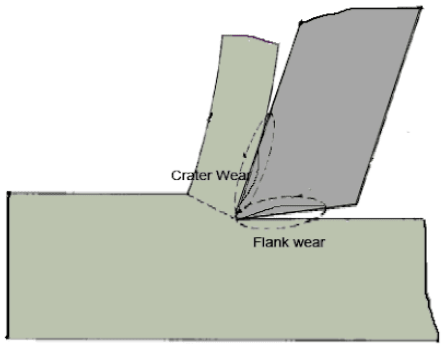

Figure 1: Flank and crater wear [4]

Garakh M. Wani and Nilesh C. Ghuge[5] In International Journal of Informative and Futuristic Research explain that cutting tools experience a variety of wear mechanisms under extreme conditions, including elevated temperature, high pressure, rapid sliding velocities, and mechanical or thermal shocks. These wear mechanisms can manifest in various forms, including the britttle crack, the flank wear, the fatigue crack, plastic deformation, crater wear, insert breakage, thermal crack and built-up edges. A primary mode of wear is contingent upon a particular cutting conditions. Flank and crater wear are the most occuring types of wear. They concluded that since single-point cutting tools is crucial due to their considerable involvement in the machining process, it is important to maximize their performance and longevity. It is necessary to analyze it both statically and thermally. Due to increased friction and depth of cut, thermal stress is created along the tool. Numerous researchers are working on this to increase longevity and efficiency. They are setting up experimental setups with various models and conducting various analyses using various cutting fluids. However, there is still much work to be done.

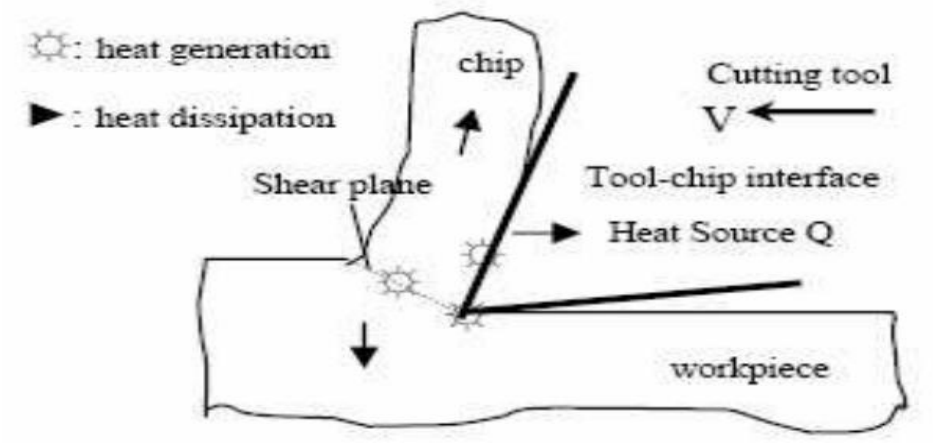

Figure 2: Heat generation and dissipation zones in the metal-cutting process[5]

M.Bourdin, L. Zouambi, M. Beida et al.[6] In Determination of a wear law for uncoated cutting tools, found that Multiple types of wear can happen at the same time: thermomechanical wear (fatigue), electrochemical wear (oxidation), thermochemical wear (diffusion), and mechanical wear (abrasion and adhesion). Adhesion wear decreases as cutting speed increases, while all other types of wear rise. To show how the cutting conditions and cutting forces produced during the machining process affect the wear phenomena, they conducted a specific number of machining experiments along with experimental measurements. As a result, the wear analysis revealed that, at rapid cutting rates, diffusion wear is the cause of the craterization of the cutting face (with little contribution from the other abrasion and adhesion wear types). The primary cause of the characterization at low cutting speeds (V < 3 m / s) is abrasion wear.

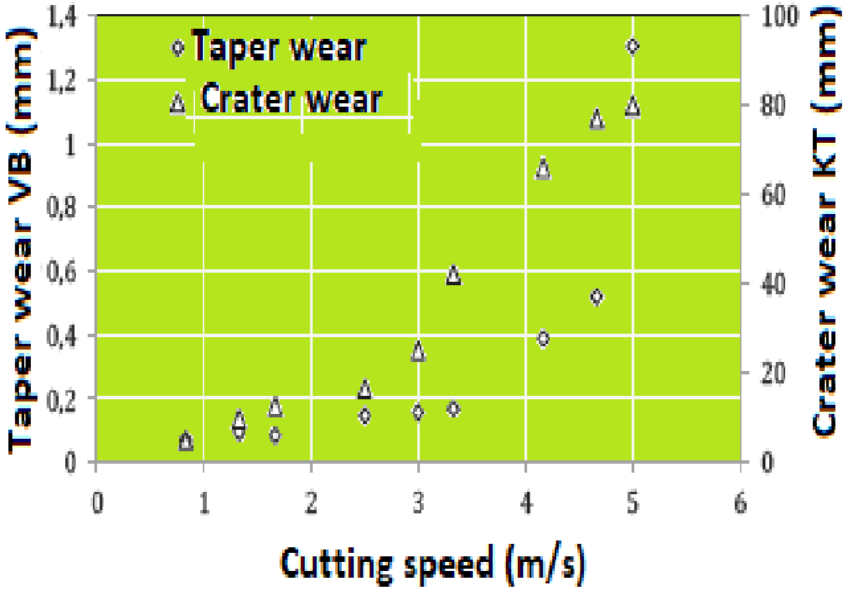

Figure 3: Evolution of the undercut wear VB and the crater wear KT as a result of the cutting speed V for f=0.15 mm[6]

Mohsen Soori et al. [3] have researched techniques for forecasting and reducing the deterioration of cutting tools throughout machining operations. In predicting the cutting tool wear during machining processes, they have utilized a range of methods such as Artificial Neural Networks, machine learning systems, temperature analysis, image data processing, finite element methods, energy considerations, multisensor fusion, support vector machines, Gaussian process modeling[3]. The researchers have discovered six main wear mechanisms that cause tool wear during metal cutting: Thermal fracture, abrasions, attrition, plastic deformation, diffusion, and grain extraction. Their proposal suggests that incorporating the algorithm for tool wear identification into smart manufacturing systems and Industry 4.0 settings can improve part production efficiency by minimizing cutting tool failures during machining processes. It is crucial to precisely anticipate the deterioration of tools during machining to replace the cutting tool before significant harm to the surface of the workpiece [3]. The capacity to assess tool wear is essential to guarantee the production of a high-quality workpiece[3].

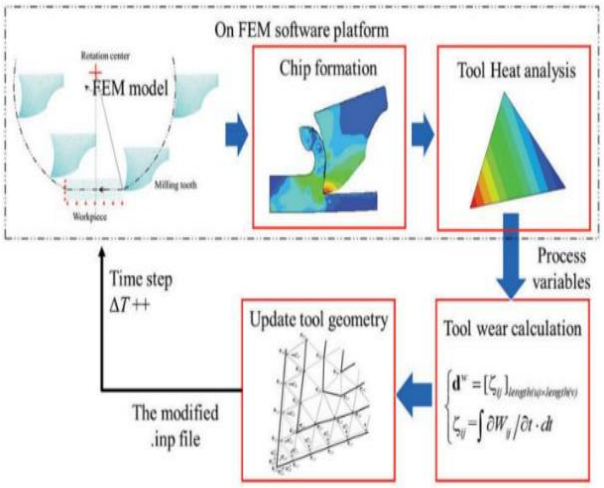

Figure 4: Tool wear prediction in FEM model[3]

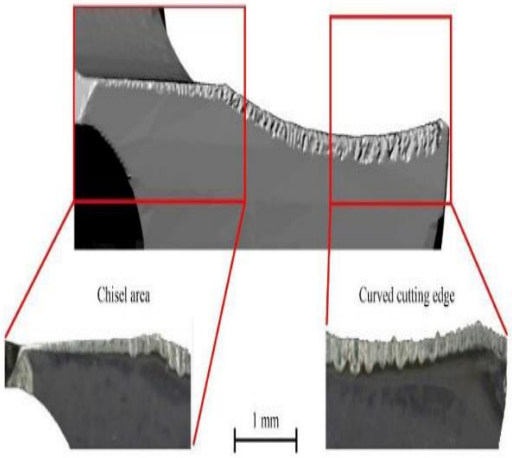

Figure 5: A simulated(left) and an experimental(right) tool wear in drilling [3]

Karem, B. and Idris M conducted a study to investigate the hardness of selected high-speed steel (HSS) and high-carbon steel (HCS) single-point cutting tools, both with and without the use of cutting fluid. A tool wear prediction model was developed using measurements of flank wear hardness (hardness of the tip) at preset machining parameters, including feed, speed, cutting mode, and cutting tool operating duration [2]**.** The Rockwell hardness of the tooltips was measured at different stages of the machining process, and the corresponding cutting parameters were recorded. The turning operation continued until the tool became completely worn out. Subsequently, multiple regression analysis was employed to model the relationships between hardness, machining time, feed, and speed, with and without coolant. They found that the model could help replace insufficient and expensive traditional tool monitoring systems and imaging technologies when it comes to tracking tool wear in developing nations [2]. Monitoring tool wear during machining processes reduces the machine failure and maximizes the profit and the productivity[2]. Using a defected tool can lead to a decline in the surface finishing and the accuracy of the

dimension of the product. To figure out the tool wear is challenging due to unpredictabilities in the cutting operations, the material and the composition of the workpiece, and the measurement taken. The stability of cutting tools is significantly affected by flank wear, reliability, and diametric precision of the machining process. Consequently, it is commonly employed as a criterion for determining the tool's lifespan.

M. Srinath, M. Pascal, And R. Nazareth conducted a static and Dynamic Performance analysis and Modal Simulation of single-point cutting tools. They used High-Speed Steel and Tungsten Carbide single-point cutting tools. They found that there is a significant drawback of High-Speed Steel (HSS) in its limited range of acceptable cutting speeds, which is considerably lower than that of Tungsten Carbide (TC)[7]. They carried out experience involving the turning process. The studies involved using various cutting speeds on aluminum as the workpiece and High-Speed Steel (HSS) as the cutting tool, which was fastened in a Dynamometer[7]. The Dynamometer was utilized to quantify the reaction forces of the individual cutting speeds, namely the feed force (FX) and the Cutting/Tangential Force (FZ). These forces were used in the FEA to conduct comparative research between Tungsten Carbide and High-Speed Steel.

The response force obtained through the data that had been recorded was utilized to perform modal, static, and Steady-State dynamic analysis. This analysis compared stress, deformation, and factor of safety (FOS) between High-Speed Steel (HSS) and tungsten carbide (TC) single-point cutting tools.

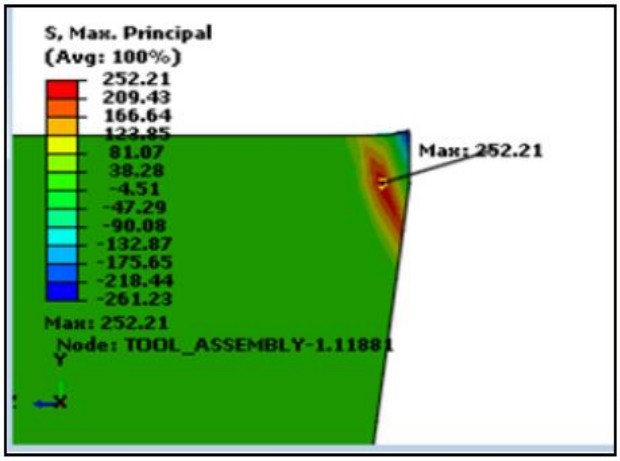

Figure 6 static load analysis for High-Speed Steel tool [7]

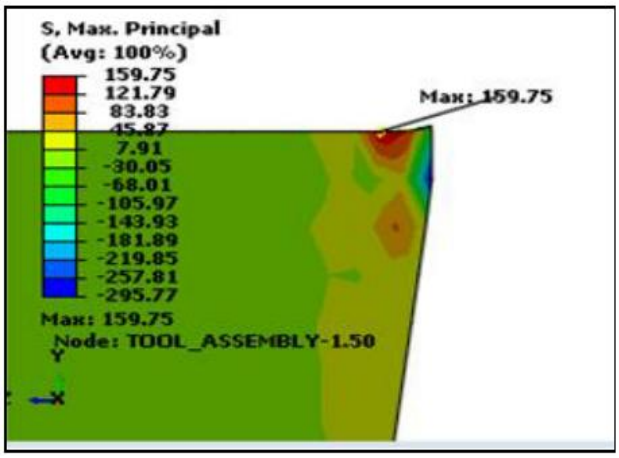

Figure 7: static load analysis for TC tool

By employing static analysis, modal analysis, and steady-state dynamic analysis, it has been ascertained that tungsten carbide (TC) single-point cutting tools demonstrate superior strength when exposed to high cutting or machining rates in comparison to High-Speed Steel (HSS) single-point cutting tools**.** Consequently, the Tungsten Carbide (TC) single-point cutting tool surpasses the High-Speed Steel (HSS) single-point cutting tool in performance. [7]

D.Yahya, Aslan E. AND C. Necip conducted a study on thermal analysis that calculates the temperature distribution based on cutting conditions in orthogonal metal cutting. They used numerical solutions to solve 2D energy equation numerically for entire cutting field, which encompasses the work piece, chip, and tool. The Finite volume method was utilized to make the study successful. The model involves the input of heat generation. The heat generation was determined by multiplying the cutting force by the cutting speed. It was discovered that the highest temperatures were seen around the midpoint of the region of contact on the edge of the cut, specifically in cases with lower cutting speeds. Increasing the cutting speed of the tool, and feed rate with cutting depths results in an elevation of tool temperature, thereby diminishing the lifespan of the cutting tool[8]

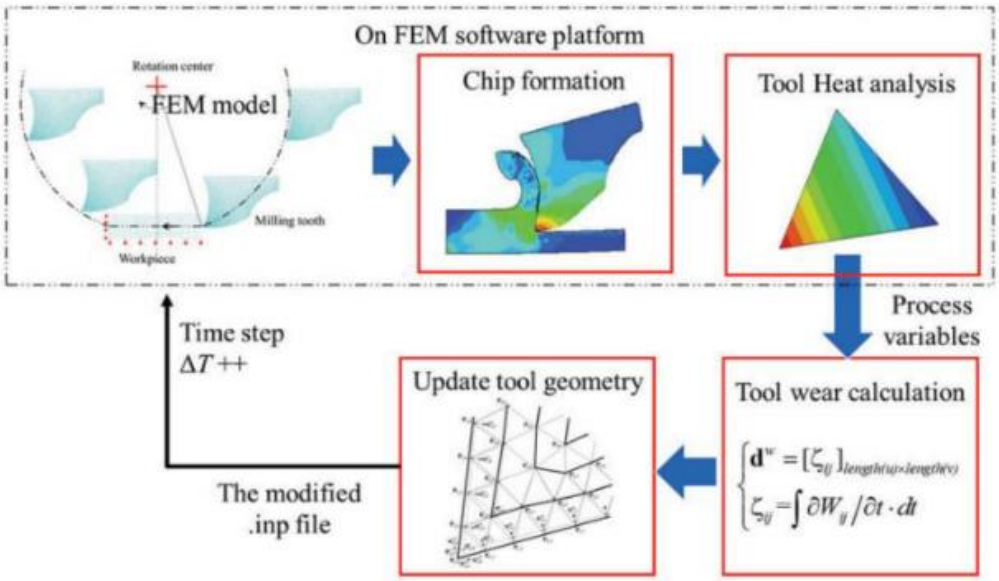

Figure 8: Finite element method[3]

Adan J., Mohamad Min. and Nizam[8] conducted a study on selecting the best parameters to minimize the cutting temperature of Mild Steel. The study was centered mainly at the temperature produced in two specific areas of heat: the primary heat zone, often referred to as the shearing zone, and the secondary deformation zone, which is the tool chip interface zone. The researchers introduced two important objective functions to optimize the issues related to the temperature induced during machining. Their comprehensive research analysis indicated that the feed rate has a substantial effect on the temperature of both the shear zone and the chip-tool interface zone, surpassing the impact of other factors. Their investigation also found that most optimization methods to far have focused on optimizing parameters other than cutting temperature.

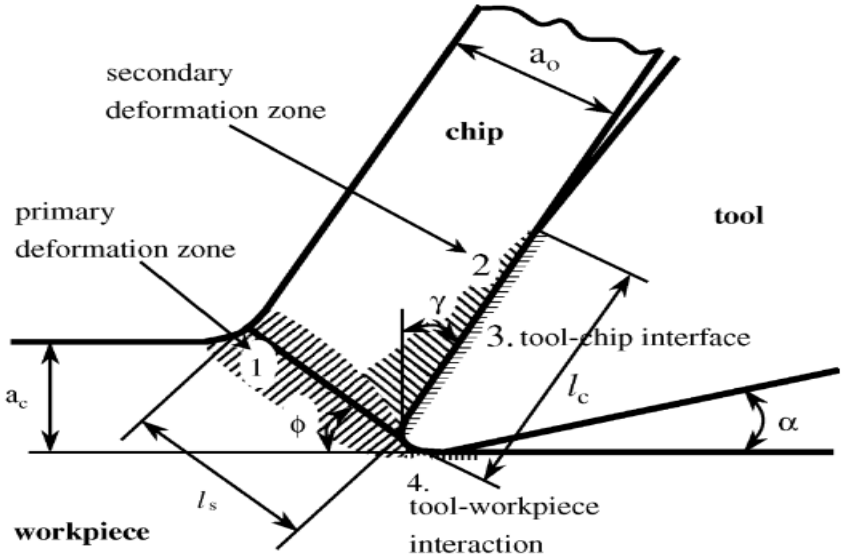

Figure 9: Schematic of orthogonal metal cutting[9]

Chinmay D. [10] Investigated the enhancement of the rate at which material is removed during machining. He explained that the cutting force is most affected by the depth of cut, followed by feed rate, while the velocity of cutting has the least significant impact. The surface finish is highly impacted by the feed rate when it is adjusted based on the nose radius. The cutting speed exerts the significant impact on the temperature generated in the cutting zone during machining. Given the aforementioned factors, the tool designer must make a judicious tradeoff in order to achieve optimal machining performance within the specified conditions.

Tangential cutting force Pz, this force is applied tangentially toward the rotating workpiece and is also referred as the turning force[11]. It is considered the greatest force component among all other forces. Tangential cutting force bears at least 99 percent of the total power desired by the cutting tool.

Longitudinal cutting tool also known as the Feed force, Px is applied perpendicularly toward the axis of rotation of the workpiece[11]. Its mean value is considered to be 40 percent greater than the magnitude of the tangential force, Pz. Subsequently, the power desired is usually 1 percent of the total because the feeding velocity is very low.

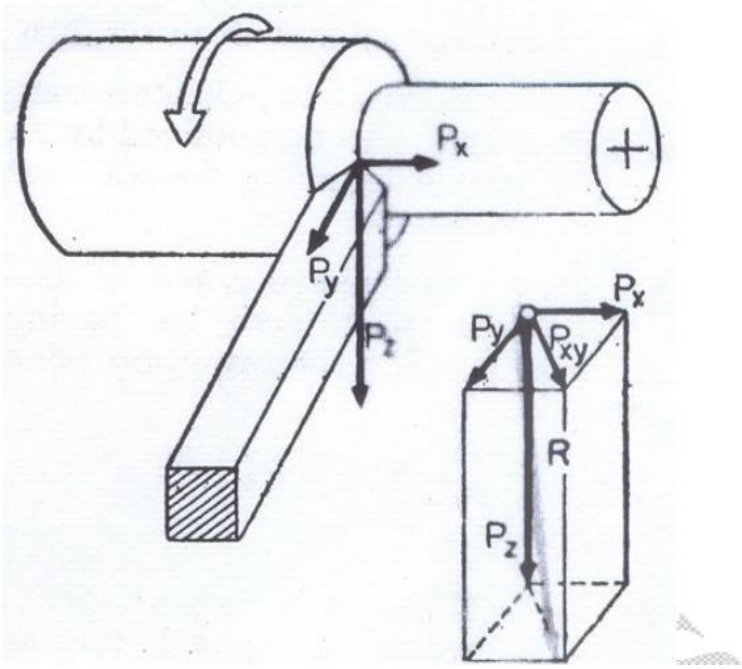

Figure 10: Cutting force in the turning process[10]

The temperature at which the cutting occurs impacts the rate at which the tool wears down. Consequently, any intervention aimed at lowering the cutting temperature would also lead to a reduction of the tool wear. Increased friction intensifies the temperature, hence promoting the deformation of the workpiece due to the thermal effect. The solid components of the workpiece underwent erosion and diffusion into the chip material, resulting in an escalation of crater wear.

While undergoing the machining process, the cutting tool directly engages with the workpiece material. Chips are formed by the process of shearing the workpiece material, which results in the generation of heat due to the plastic deformation of the work material and the friction between the workpiece and the tool. This heat is then transferred to the cutting tool [8]. When the cutting situation grows rapidly, both the cutting tool and the workpiece experience a significant temperature rise.

The use of an empirical methodology to comprehend and forecast the deterioration of tools arises due to the incapacity of witnessing directly the underlying theories and accurately investigating the specific patterns responsible for tool wear. The purpose of this study is to uncover the underlying causes of tool wear for researchers in this field.

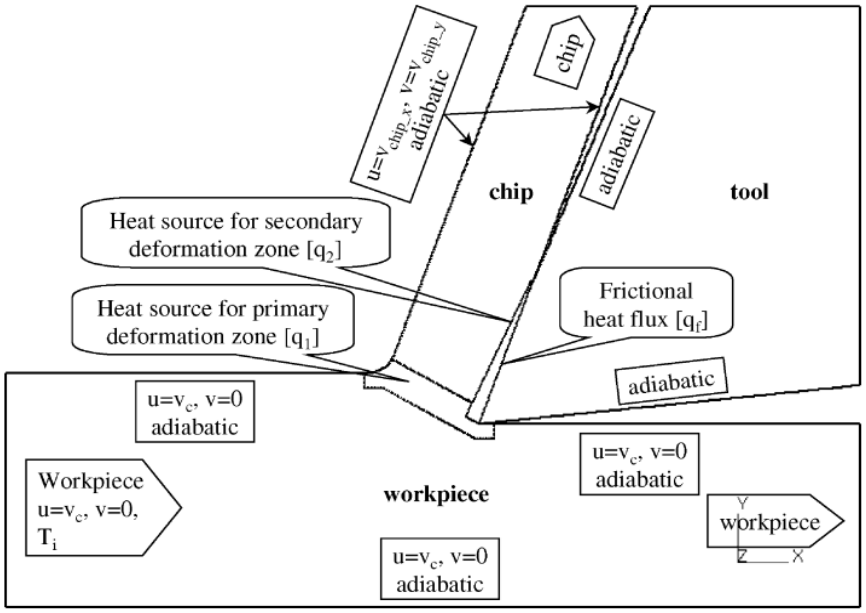

Figure 11: Boundary condition used in the thermal model

Astakhov[8] developed a model to accurately compute the distribution of temperature and thermal energy in the deformation zone, by emphasizing that there is a transformation of the mechanical energy involved in the material removal process to thermic energy, the equation of the heat involved becomes a crucial focus in studies on metal cutting [12]The given equation can be expressed as below:

$$\mathbf{Q_E = F_C V_C = Q_C + Q_W + Q_T}\ [12]$$

Where in this equation, we have the cutting force, F_C measured in Newton, N; the cutting velocity measured in meters per second m/s; the heat energy conveyed by the chip, measured in Joule per second, J/s; The heat energy transferred to the workpiece by conduction $Q_{W,}$ measured in Joule per second J/s; and The rate at which thermal energy is transferred to the tool $Q_{T,}$ measured in joules per second (J/s).[12] The cutting tool has direct contact with the work material. A chip is produced through the shearing process of the workpiece, during which the heat involved from the plastic deformation of the work material and the sliding effect occurring in the workpiece and the cutting tool is transferred to the cutting tool

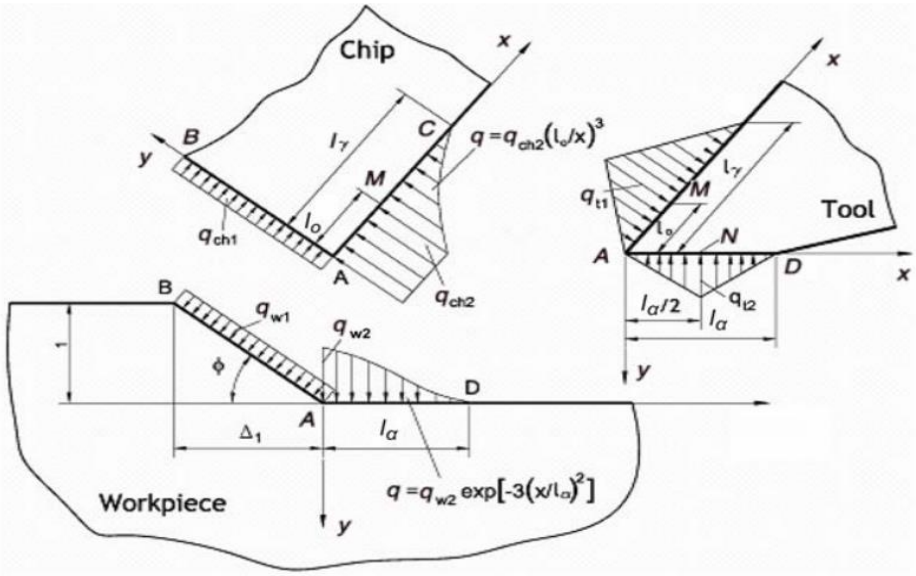

Figure12: The model developed by Astakhov which investigates the thermal effect occurring during machining.[12]

2.2 Overview on different cutting tool wear patterns

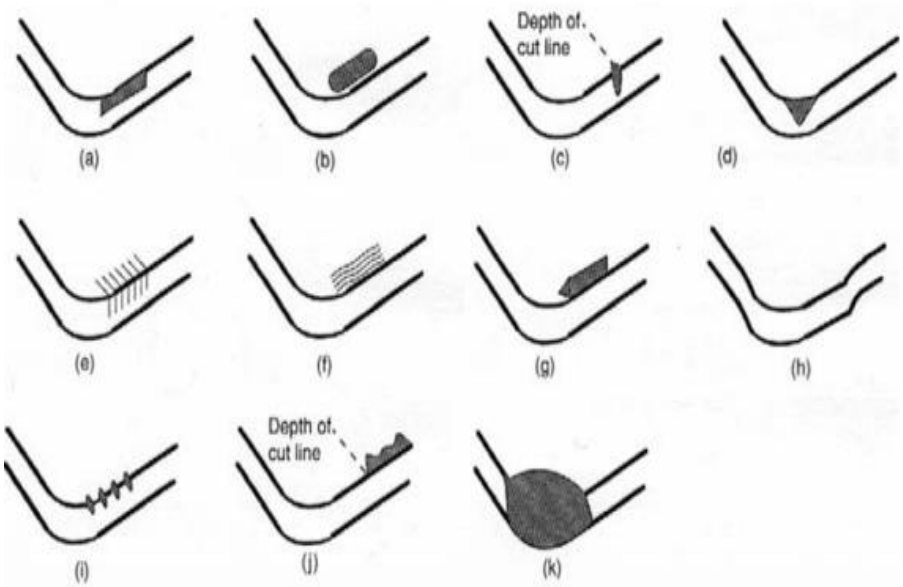

Figure 13: Types of tool wear[12]: (a) Flank Wear, (b) Crater Wear, (c) Notch Wear, (d) Nose Radius Wear, (e) Thermal Cracking, (f) Parallel Cracking, (g) Built-Up-Edge, (h) Gross Plastic Deformation, (i) Edge Chipping, (j) Chip Hammering, (k) Gross Fracture

2.2.1 Flank wear

Flank wear occurs when a machined workpiece surface and the tool flank experience friction, resulting in the development of a worn area known as a wear land. [4]. This wear land's width, VB, serves as a measure of flank wear, significantly impacting the mechanics of cutting. Flank wear causes a significant rise in cutting forces [4]. If the level of Flank wear overtakes the optimum threshold (VB greater than 0.5mm to 0.6 mm), the increased Cutting Force can result in tool wear.

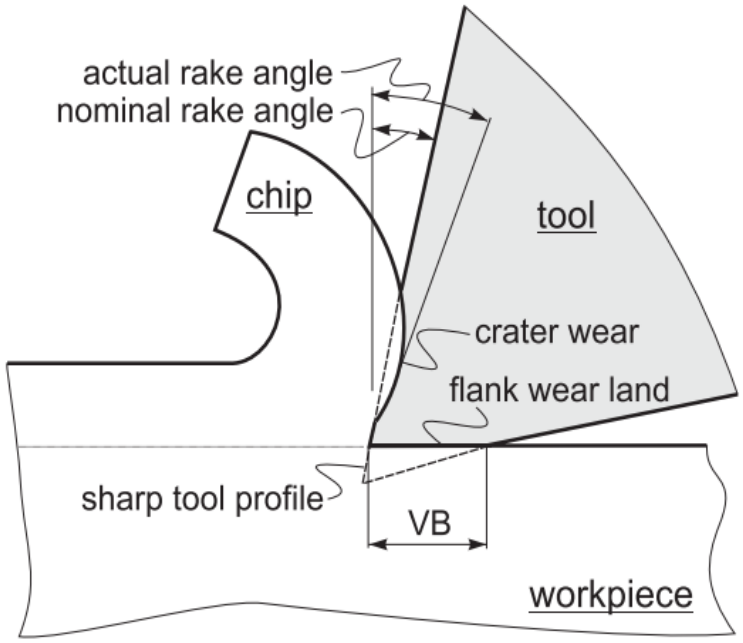

Figure 14: Cross-sectional view perpendicular to the main cutting edge of a worn cutting tool representing the effect of crater wear on a tool rake angle and the flank wear land[4]

The lifespan of the cutting tool has a direct impact on the production cost of the application firms as it is a consumable product. Therefore, enhancing the longevity of the tools is a subject that is often shared among professionals in the manufacturing sector [13].

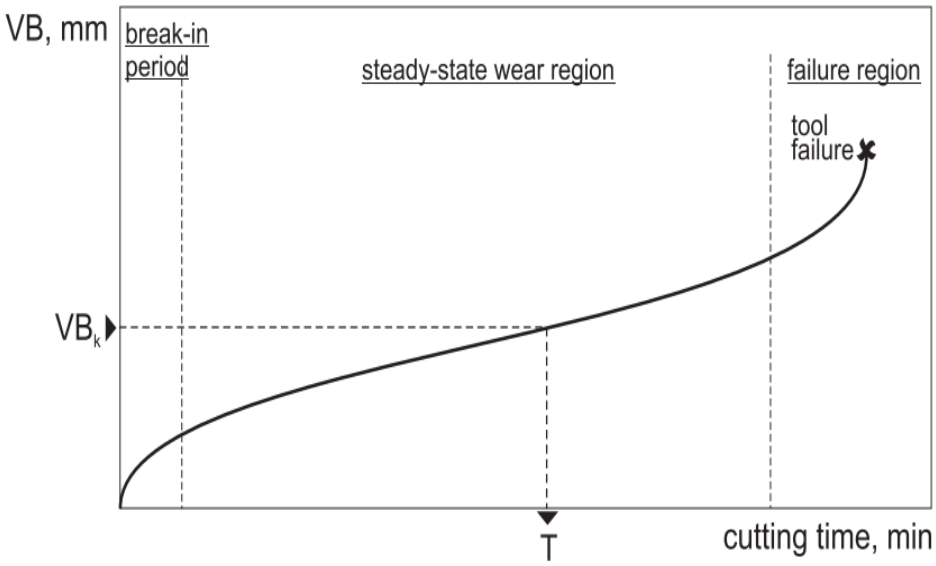

Figure 15: The wear land versus Cutting time [4]

2.2.1.1 Characteristics of Flank wear

I. It represents the primary form of wear observed at the side parallel surface to the cutting edge, typically arising from the abrasive or adhesive wear between the cutting edge and the machined surface.

II. It frequently arises as a result of high temperatures that affect the characteristics of both the tool and the work material.

III. It results in the formation of a worn area, and the consistency of this worn area may differ along both the primary and secondary cutting edges of the tool.

IV. Measurement is achieved with a help of the average wear land size and the optimum Wear Land Size (VB_{max}).

V. The concept is elucidated by employing an Equation for the expectancy of the tool lifespan.

VI. Flank Wear can be explained by the use of the equation for the tool life expectancy which is defined as: $\mathbf{V_cT^n=C}$. However, a suitable encompassing version of the equation is

$\mathbf{V_cT^nD^xF^y=C.}$ **(**prior to the depth of cut and the feed rate**).**

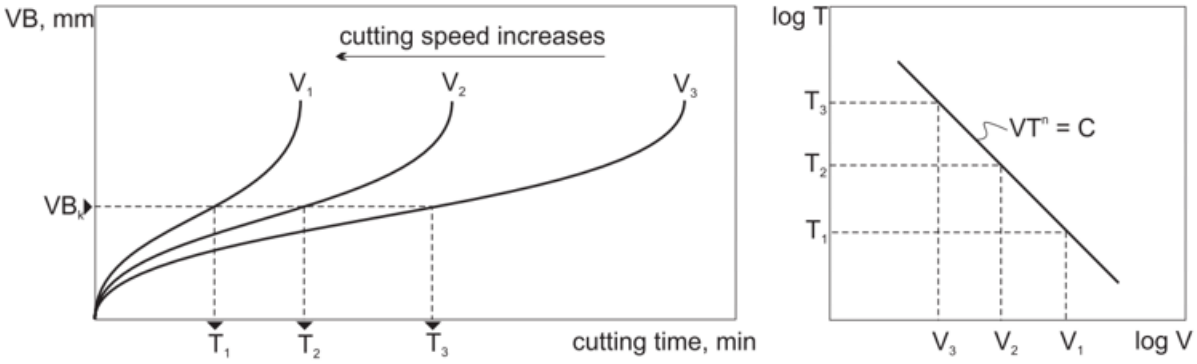

Figure 16: Various cutting speeds affect wear land and tool life (left side) and The correlation between the logarithm of cutting speed and tool life (Right side)[4]

V_c is the cutting speed, T is the tool life, D is the depth of cut, F is the feed rate (mm/rev, or inch/rev), **x** and **y** are exponents established through experimental means for each cutting scenario, C is the machining constant, Determined through experimentation or information available in published data books, it generally relies on the characteristics of tool materials, workpiece, and feed rate, the value of n is exponential. The range of values for n is 0.1 to 0.15 for HSS tools, 0.2 to 0.4 for Carbide tools, and 0.4 to 0.6 for ceramic tools.

2.2.1.2 Reasons of flank wear

I. An increased cutting speed results in a swift increase in flank wear.

II. Increasing the cut depth and feed can result in an enlargement of the flank wear.

III. Workpiece abrasion caused by rigid particles.

IV. The disengagement of small-scale fusion joints created between the tool and the workpiece

V. The gradual erosion caused by small pieces of accumulated material on the cutting edge, which collide with the exposed surface (flank face) of the tool.

2.2.1.3 Strategies for mitigating the Occurrence of flank wear

I. Decrease cutting velocity
II. Decrease feed rate and cutting depth
III. Utilize a high-grade carbide if available.
IV. Employ chip breakers to prevent the production of built-up edge.

2.2.1.4 The consequences of flank wear are twofold:

I. The cutting force becomes high
II. The component's surface roughness has increased.
III. Flank wear has an impact on the precision of the workpiece's dimensions.
IV. If the form tools are utilized, the occurrence of flank wear will lead to a modification in the configuration of the manufactured components.

2.2.2 Crater wear

Crater wear refers to the erosion or damage that occurs on the surface of a material, typically due to repeated impacts or abrasive forces[14]. Crater wear is a phenomenon where a concave segment is formed on the tool face due to the sliding action of the chip. This wear impacts the mechanics of the process by augmenting the effective rake angle of the cutting tool, which in turn helps in the cutting operation. Concurrently, the erosion of the tool's edge, known as crater wear, reduces its strength and increases the likelihood of the tool breaking [4]. Crater wear is typically a negligible issue.

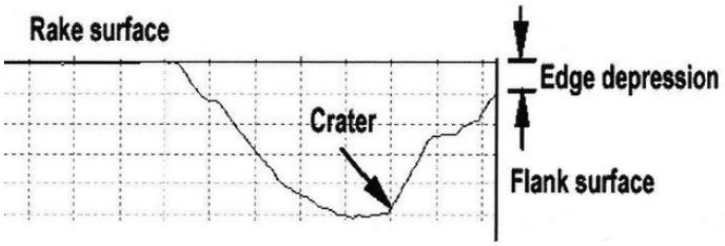

Figure 17: Crater wear[15]

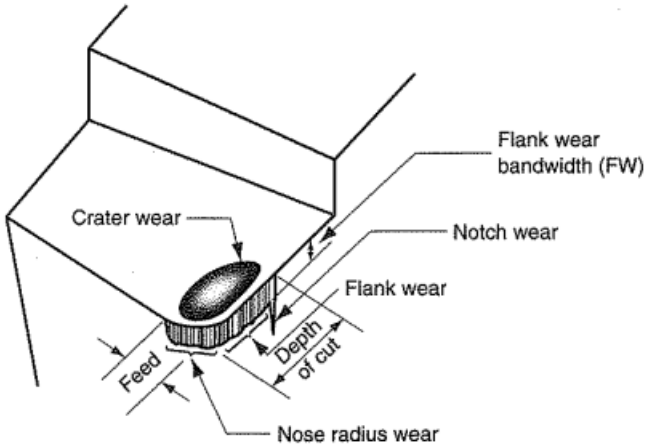

Figure 18: Diagram of a worn cutting tool showing the principle locations and types of wear that occur[16] Page 543

2.2.2.1 Characteristics of crater wear

I. Crater wear occurs when the material removed gradually erodes the rake face of the equipment.
II. The passing of chips across the rake face creates significant friction between the chip and the rake face. The friction between surfaces causes a scar to form on the rake face, usually running parallel to the main cutting edge.
III. Crater wear impacts the operating rake angle and minimizes the cutting force, while also weakening the cutting edge.
IV. It is familiar in the materials that are malleable such as steel, which produces continuous and uninterrupted chips. Furthermore, this phenomenon is frequently found in High-Speed Steel (H.S.S.) tools as opposed to ceramic or carbide tools, since the latter exhibit considerably higher hot hardness.
V. It typically appears at a depth that is approximately equal to the depth of the material being cut, indicating that its depth is essentially proportional to the cutting depth.
VI. Crater wear occurs in areas with elevated temperatures, reaching around 700°C.

2.2.2.2 Causes of Crater wear

I. Intense abrasion at the interfaces between the chip and the tool, particularly on the rake face.
II. High temperatures occurring at the boundary between the tool and the chip.
III. Increasing the feed rate causes a greater force to be applied to the tool interface, which at a time leads to a leap in temperature at the interface of the tool chip.
IV. A boost in cutting speed causes an elevated the velocity of the material being removed at the rake face, leading to a temperature increase at the chip-tool interface and subsequently, an escalation in crater wear.

2.2.2.3 Strategies for mitigating crater wear

I. The utilization of appropriate lubricants can mitigate the abrasion process, leading to a reduction in crater wear.
II. Using a suitable coolant helps to quickly dissipate heat from the tool-chip interface.
III. Reducing cutting speeds and feed rates
IV. Employing tools composed of more durable materials with higher hot hardness
V. Utilize a tool with a positive rake angle.

2.3 Factors contributing to tool wear

Multiple factors contribute to the wearing down of tools. Several of them merit special discussion, as follows:

2.3.1 Abrasive wear

Abrasive wear mostly occurs due to the infiltration of inflexible particles, such as carbon nitride and oxide compounds, into the workpiece material, as well as the buildup of material on the tool edge. It is a form of mechanical wear that predominantly happens when cutting speeds are low.

2.3.2 Adhesive wear

Hot chips often adhere to the tool rake face due to the elevated pressure and temperature at the tool-chip interface. This leads to the creation and elimination of fused connections. When the welded connections detach, they dislodge fragments of the cutting tool, resulting in a wear pattern like a crater. The diagram below depicts adhesive wear.

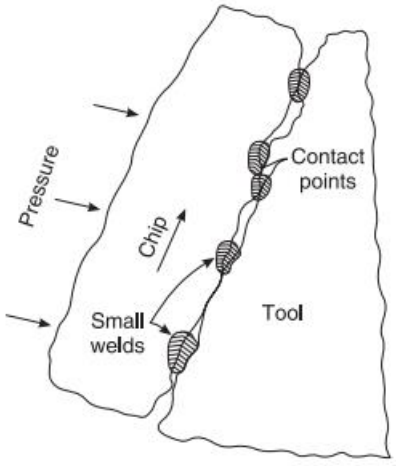

Figure 19: Showing point of contacts and metallic bonds (welds) formed between mating surfaces of chips and tool JP Kaushish page 313[17]

2.3.2 Diffusion wear

Diffusion wear is the result of an atomic exchange between the tool and workpiece materials caused by elevated pressure and temperature. The initiation of this process commonly occurs at the interface between the chip and the tool.

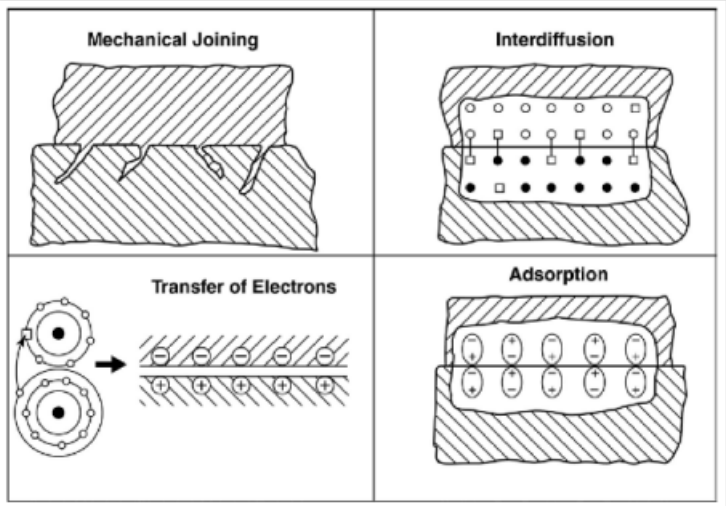

Figure 20: The effect of adhesion wear out mechanism[18]

2.3.3 Chemical wear

Chemical wear arises when material interactions with its surroundings lead to the formation of new compounds and the degradation of its surface. Various factors, including corrosion, oxidation, and erosion can trigger this.

2.3.4 Fracture wear

Fracture wear, also known as chipping or spalling, is a detrimental form of wear that occurs when the cutting edge of a tool breaks away, typically near the end or along its length. This type of wear can abruptly terminate the machining process and significantly damage the workpiece. Bulk breakage is considered the most severe and undesirable form of fracture wear, as it can completely shatter the cutting edge, rendering the tool unusable. To minimize the risk of fracture wear, it is crucial to optimize the limiting factors of machining like cutting speed, feed rate, and the geometry of the tool and employ effective coolant systems to maintain tool temperatures within safe limits.

3 Creating a 3D model of the cutting tool deformation during machining

Using the right plane, I created a rectangle of which each side was 25 mm.

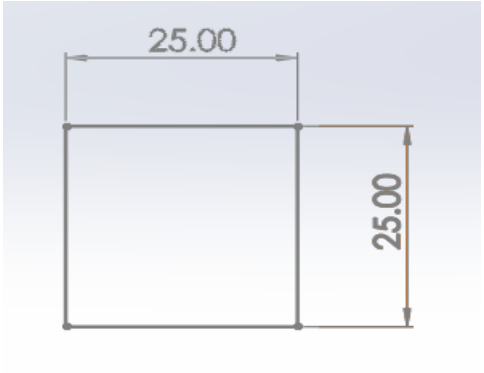

Figure 21: a created rectangle

Using the Boss-Extrude command from features, I extruded the rectangle to a length of 175 mm

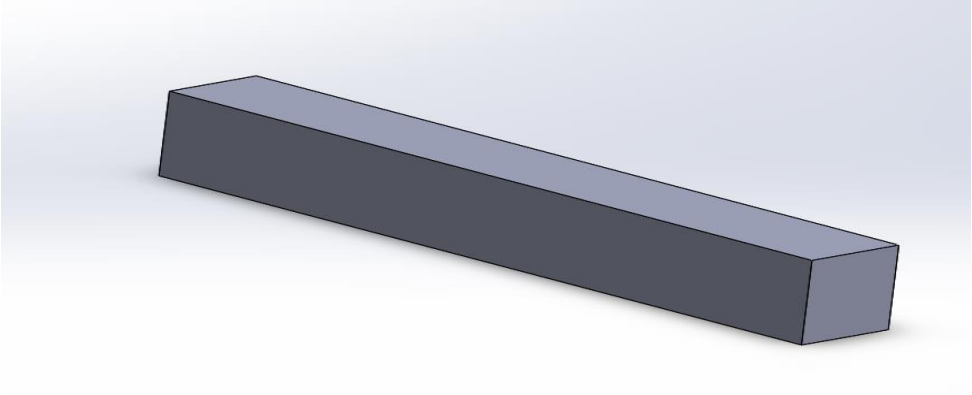

Figure 22: An extruded rectancle

The next step was to draw a line which we will use to create a split line that will help be used to remove unwanted material while also creating different cutting edges. The dimensions used are shown in the figure below

Figure 23: Applying a split line

From the line drawn, a split line is created by projection. The two lines are connected and made vertical.

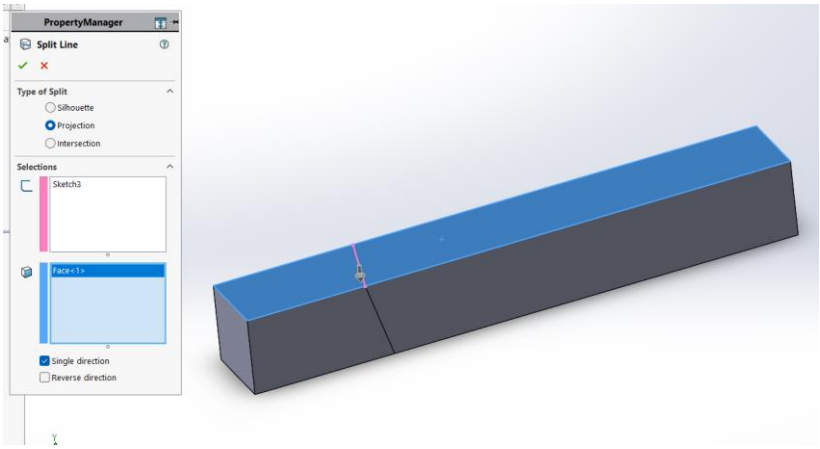

Figure 24: Creating a split line

The next is to create a side rake angle. I decided to use 20 degrees.

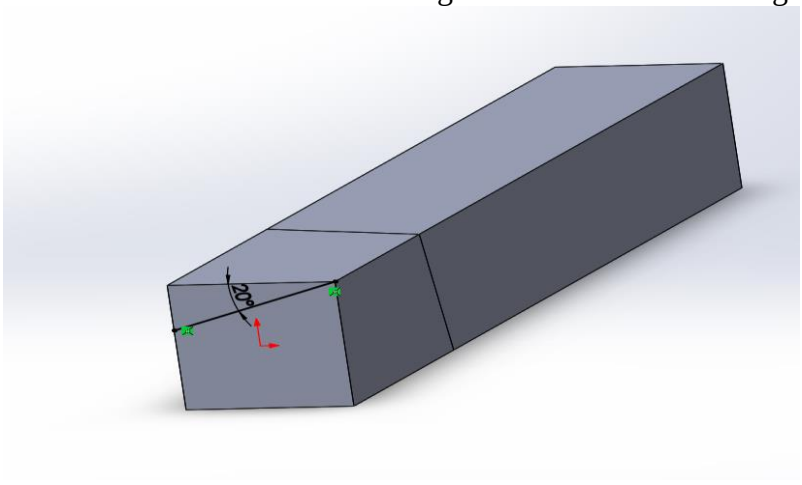

Figure 25 Creating a side-rake angle

On the other face of the workpiece, I a back rake angle of 10 degrees is drawn.

Figure 26: Creating a back rake angle

The next step is to create a plofile that has to be removed. To do this, I sketched the lines that will create the geometry of the plofile that will be removed using the lofted cut command from features. Both profiles and the loft cut are shown below.

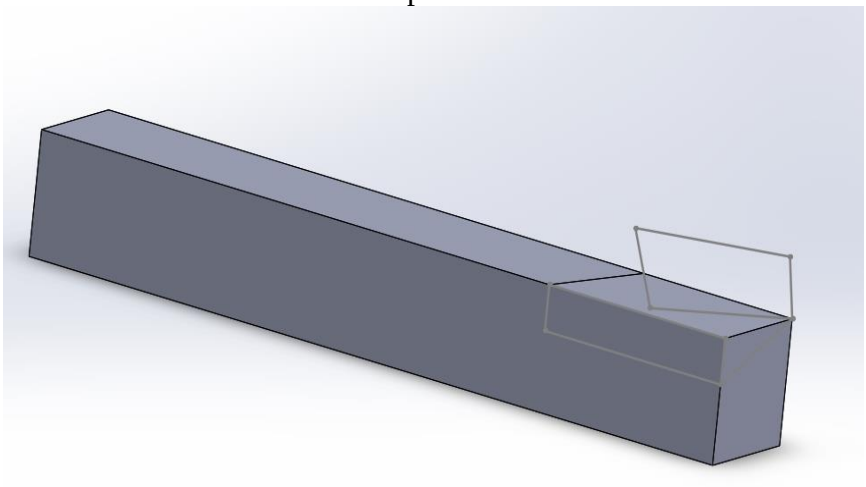

Figure 27: Creating profile and loft

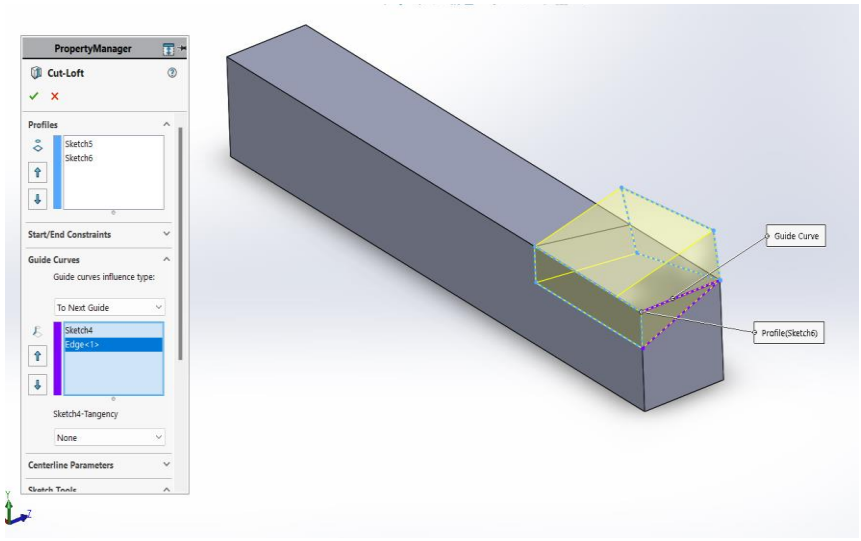

Figure 28: A created profile and guide curve

As a result, the workpice becomes like this after the removal of unwanted material.

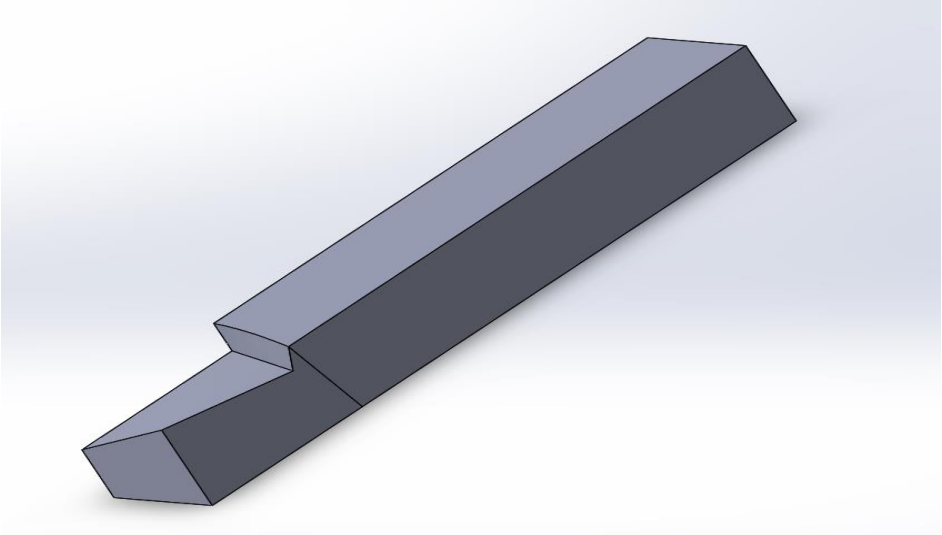

Figure 29: After removing unwanted material

The next step is to create a side cutting-edge angle. Using the draft command, A neutral plane is created perpendicular to the line that was used to create a split line. An angle is taken to be 8 degrees as shown.

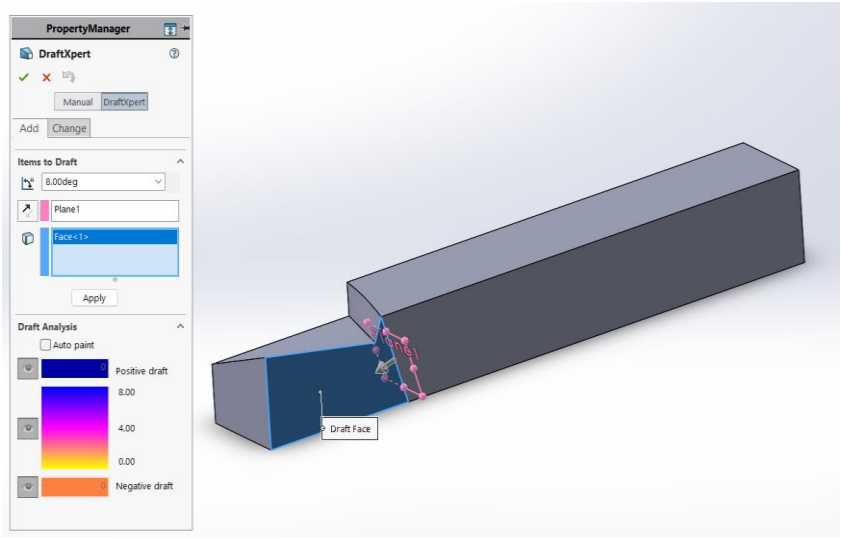

Figure 30: Creating a side-cutting edge angle

Next, A fillet of a 7 mm radius is created as shown on the figure.

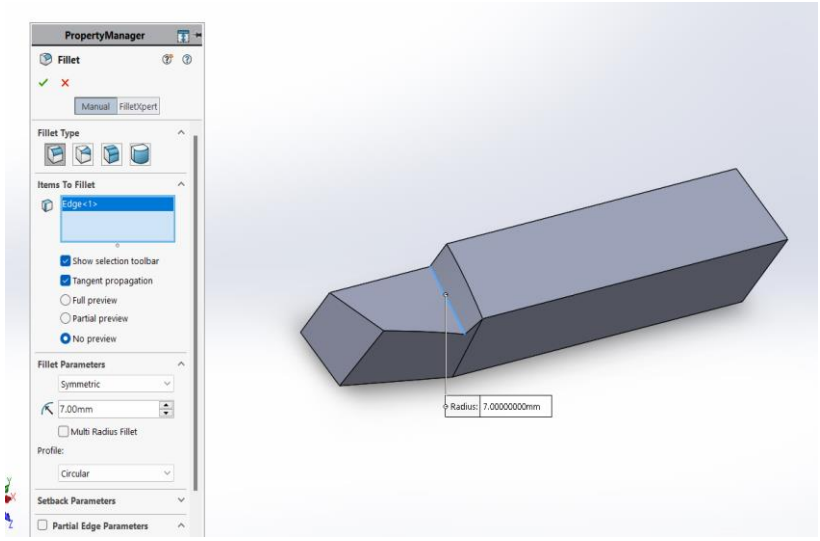

Figure 31: Created fillet

The next step is the creation of the end clearance angle. To do this, a top plane is created and using draft command the end clearance angle is created. The face is drafted to 7 mm. The process is shown in the figure below.

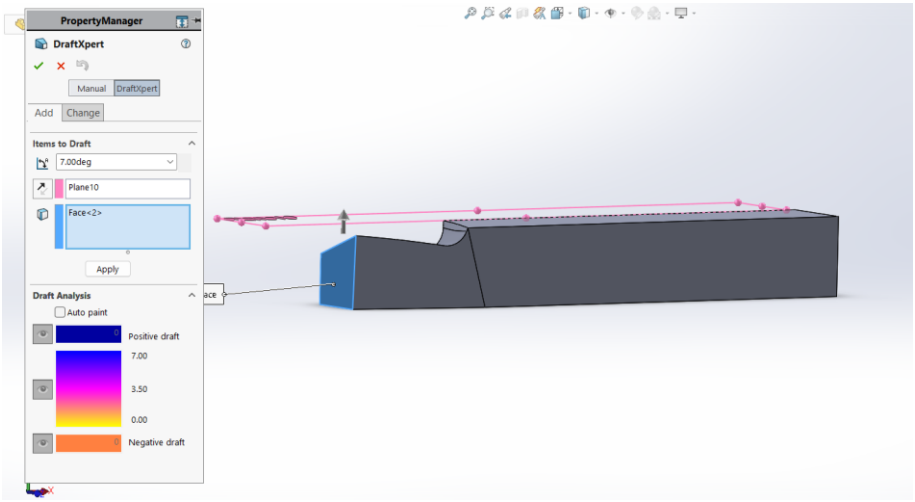

Figure 32: Using DraftXpert to create a top plane

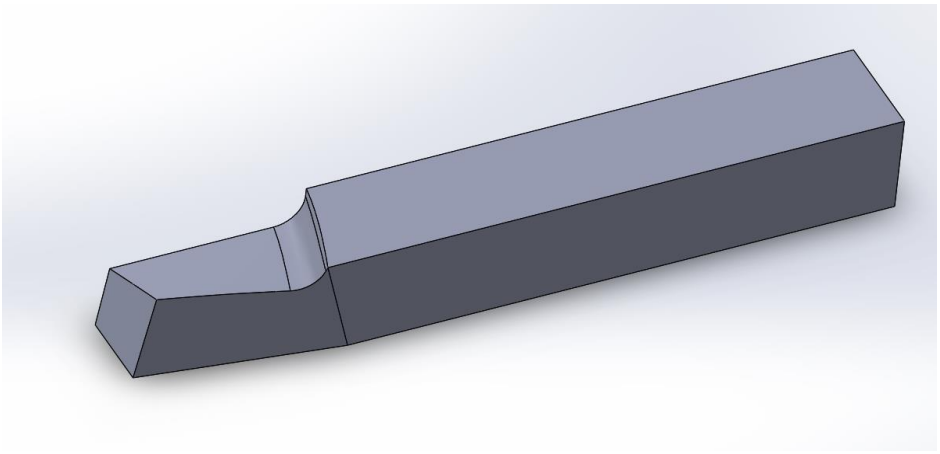

Figure 33: An End Clearance angle

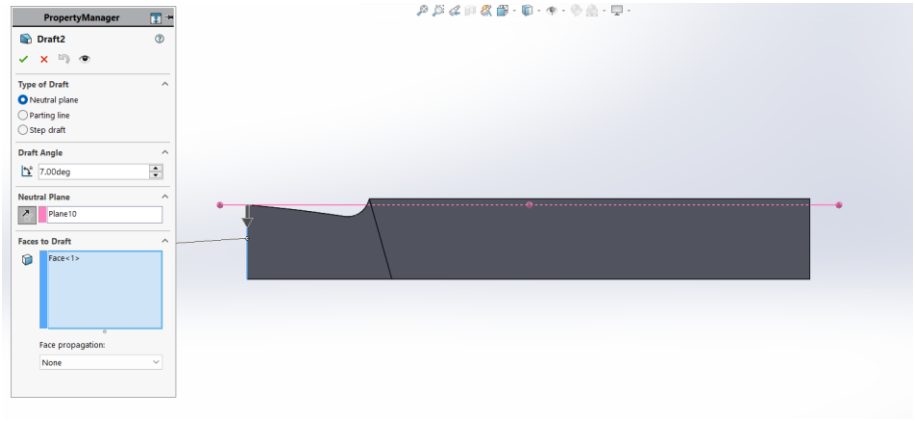

Figure 34 : using DraftXpert to create the top plane

Reversing the neutral plane direction, the end clearance angle is created

Figure 35: A created end clearance angle

The next step is to create the end cutting edge angle, the same process is used like previous angle. I decide to give it a magnitude of 7 degrees.

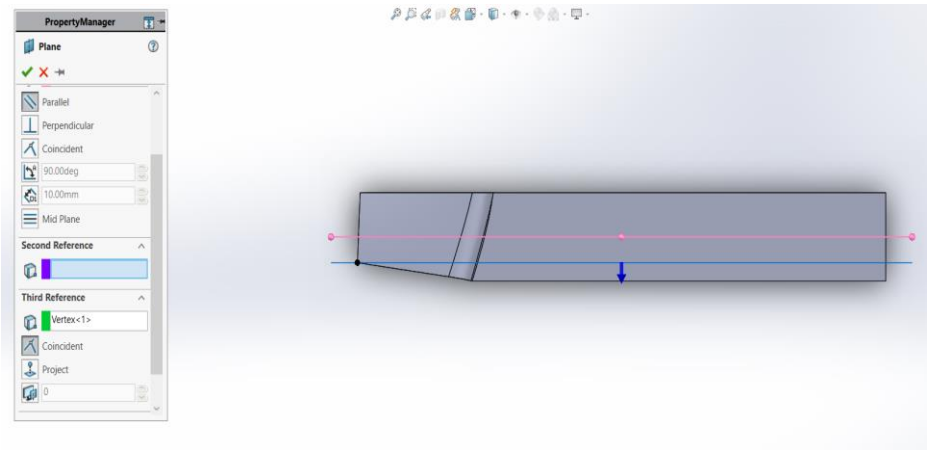

Figure 36: creating a plane on the vertex

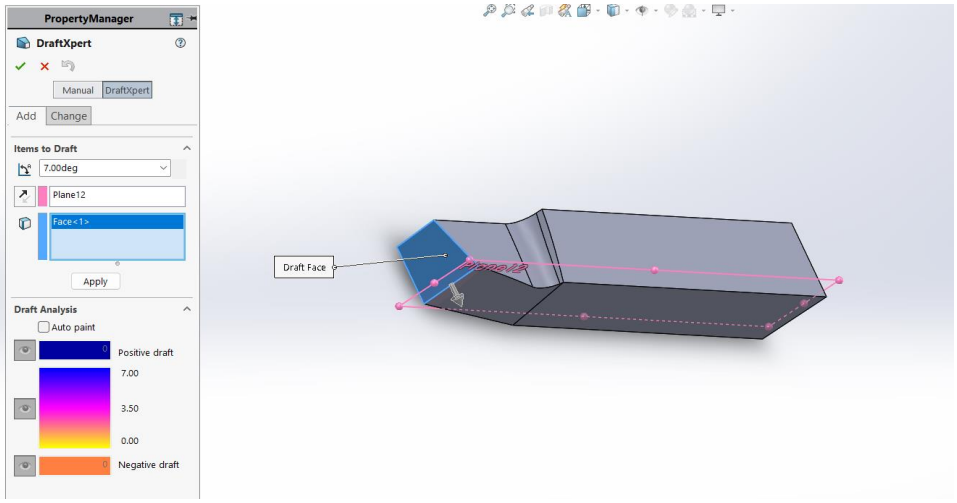

Figure 37: Using the draftXpert to create the plane

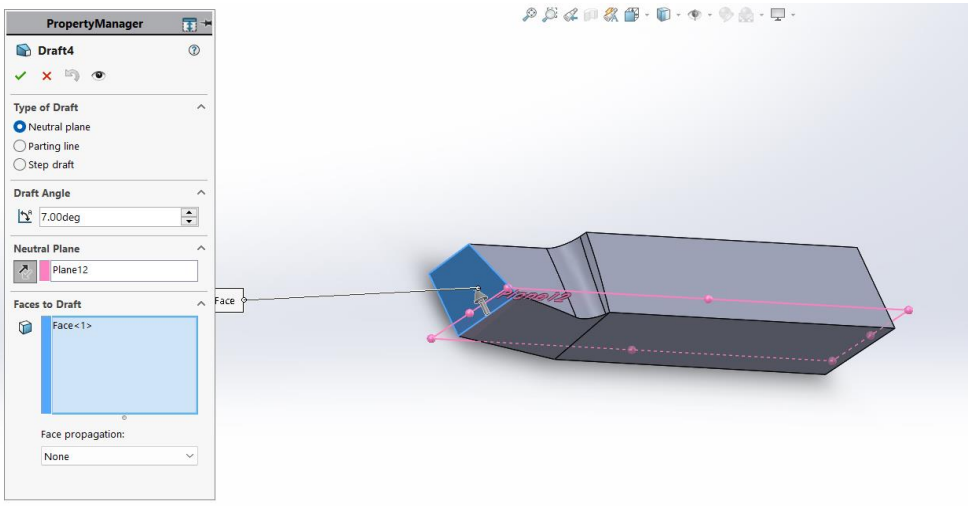

Figure 38: Reversing the direction of the neutral plane

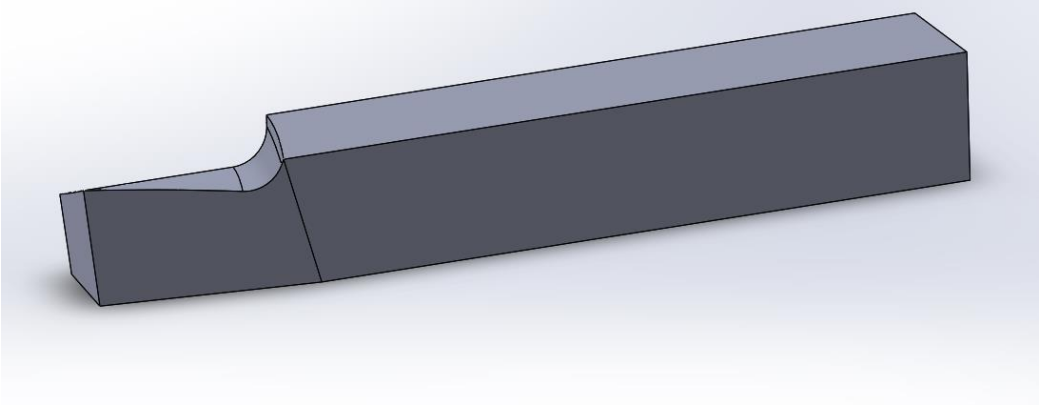

Figure 39: End cutting-edge angle

The next step is to create a nose radius. Since it is a single-point cutting tool, I decided to give it a radius of 1 mm.

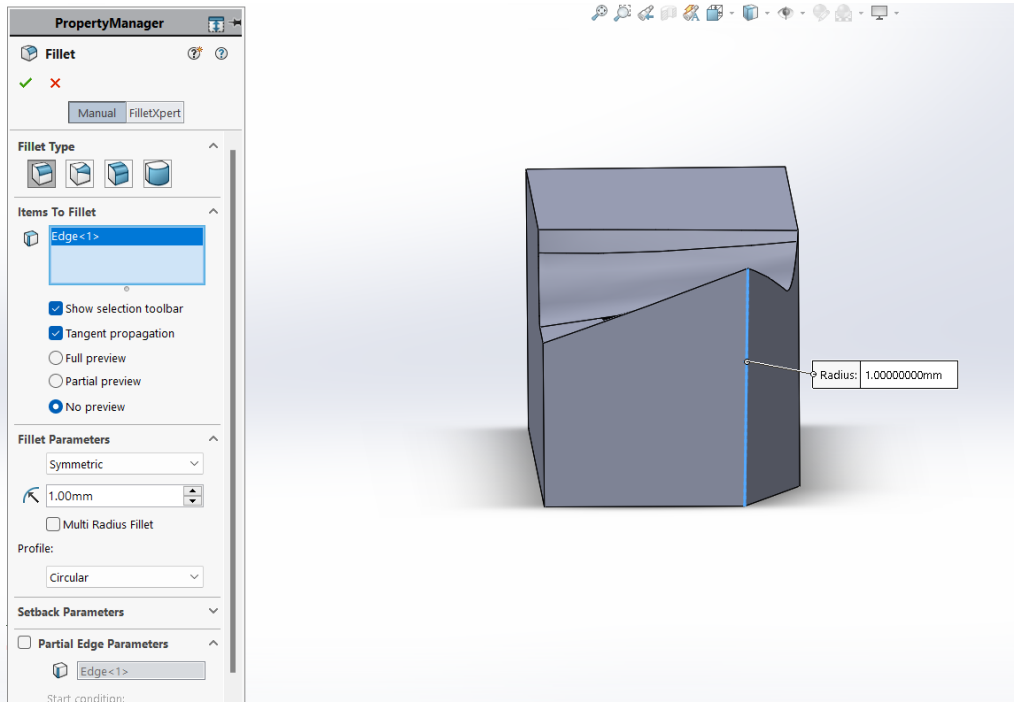

Figure 40: The nose radius

The cutting tool is now ready as it can be seen from the figure below.

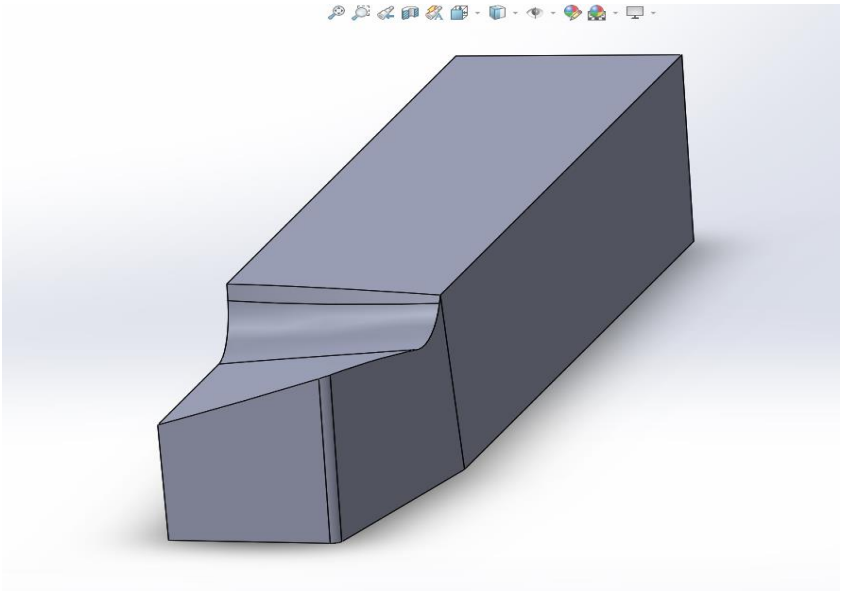

Figure 41: A single-point cutting tool

Now, I have decided to assign the material for the cutting tool. The material I used is called AISI 4340, Steel, normalized. The material properties are shown in the below table.

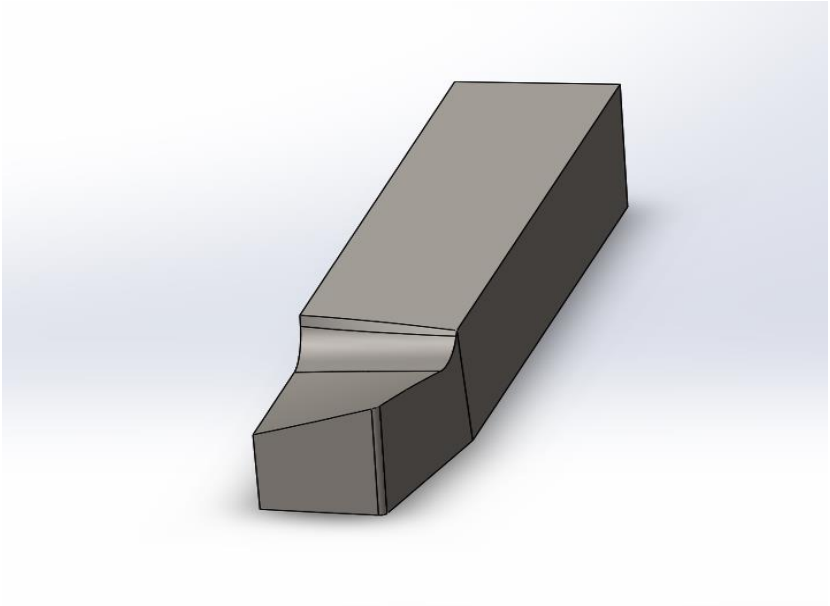

Figure 42: Material assignment of the cutting tool

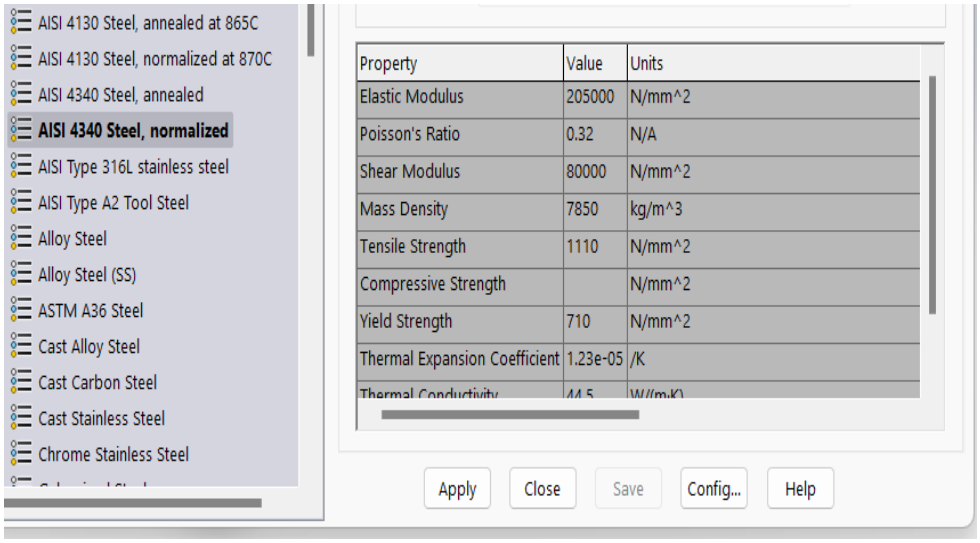

Table 1: Assigning the material for the cutting tool

The next was to draw a model workpiece as shown. It is a cylindrical workpiece created by revolving

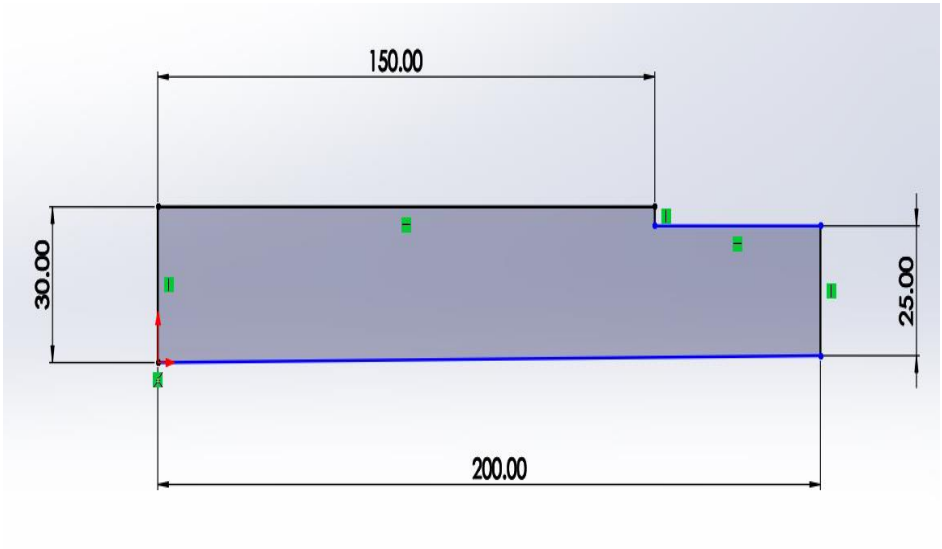

Figure 43: A workpiece geometry

The revolved workpiece can be shown below, The material is alloy steel, Its properties are given in the table below:

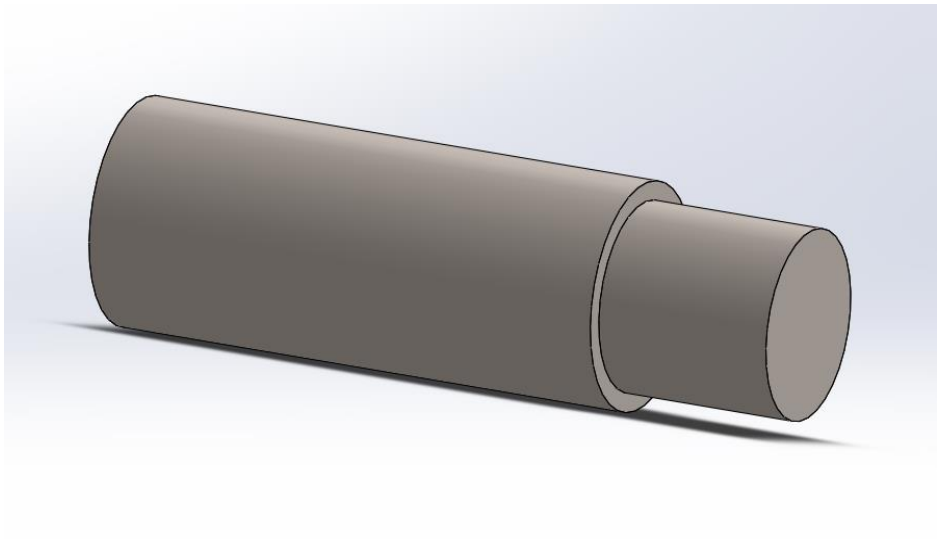

Figure 44: A cylindrical workpiece

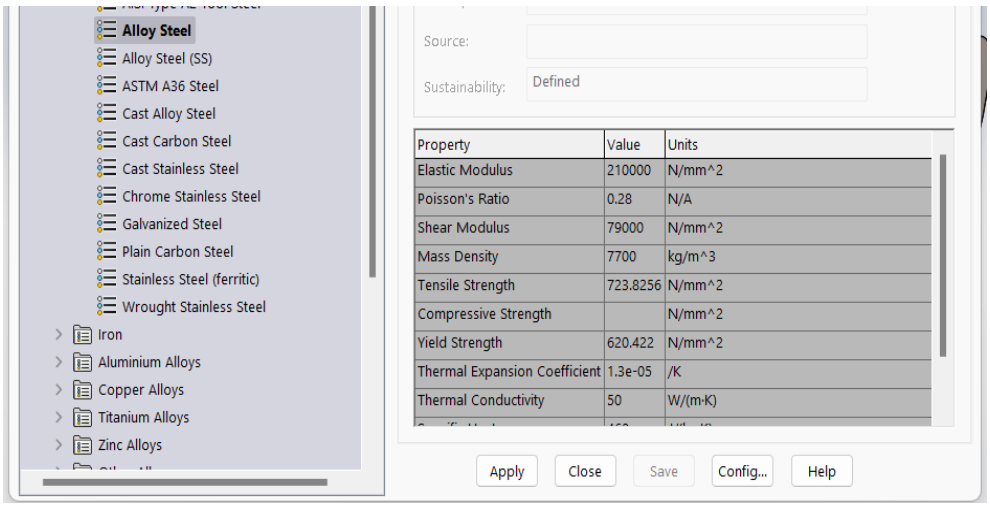

Table 2: Material property for the workpiece

Since we have the cutting tool and the workpiece, An assembly of the workpiece and a single-point cutting tool is created. This assembly will be used to analyze the wear patterns in machining.

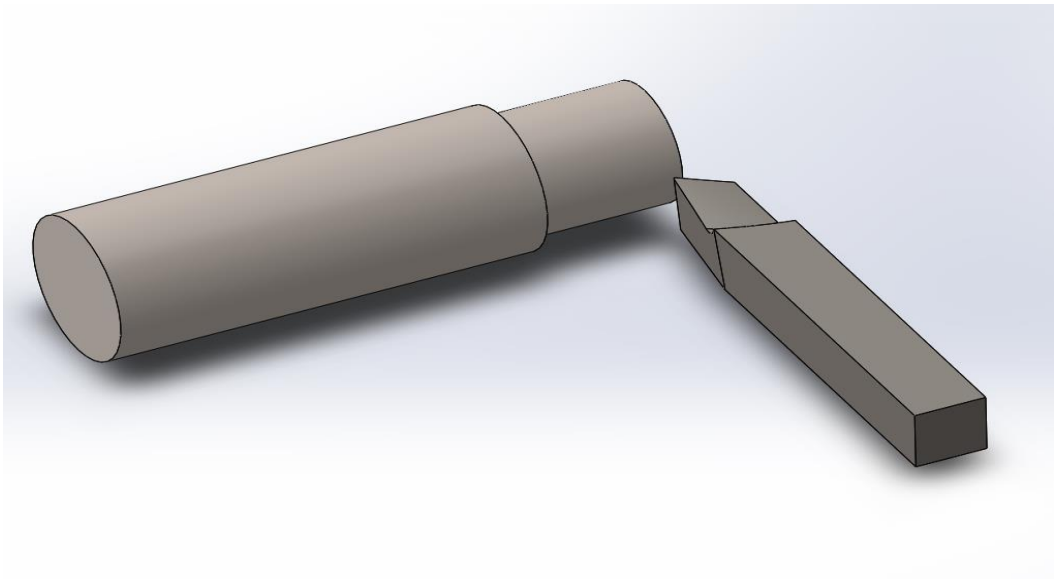

Figure 45: A 3D model assembly of the cutting tool and the workpiece

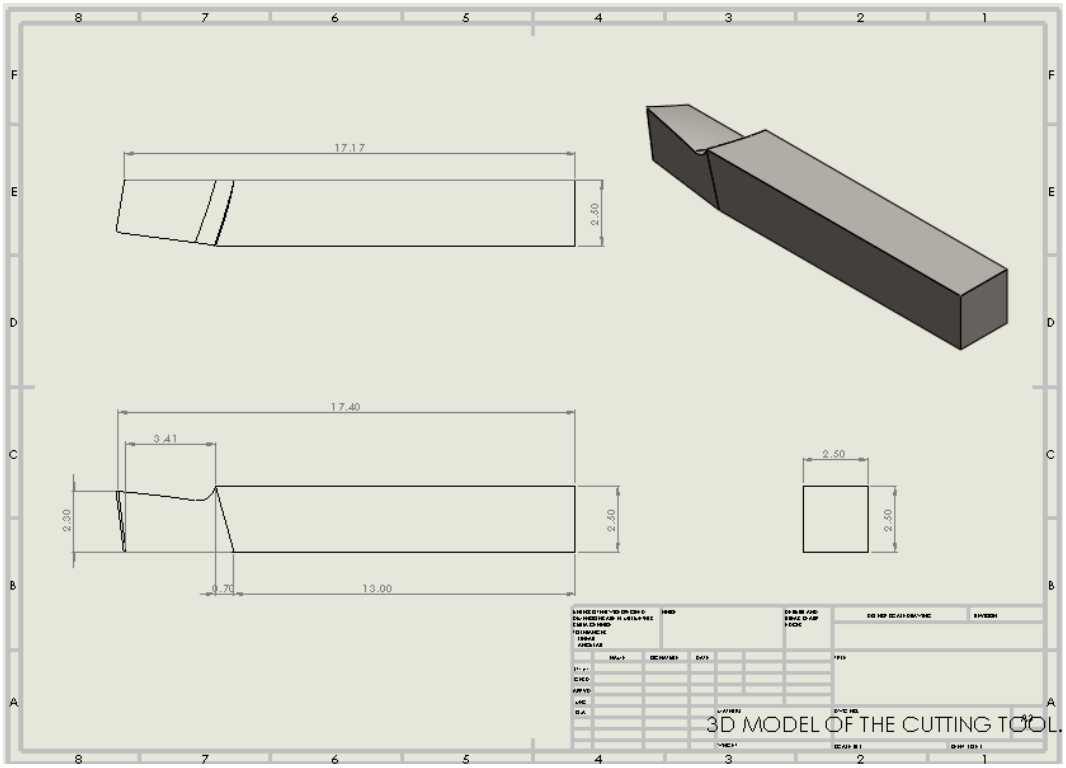

Figure 46: A draft assembly of the cutting tool

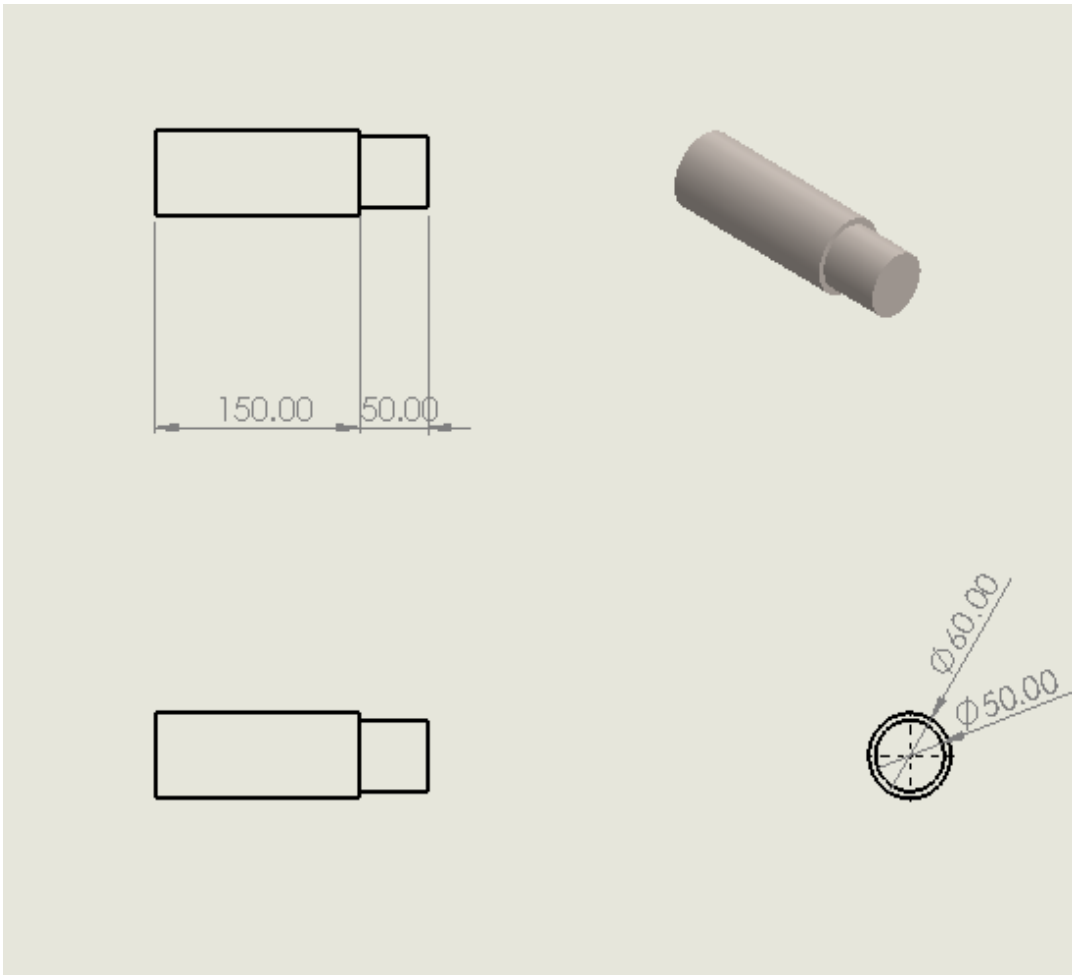

Figure 47: A draft assembly of the workpiece

4 Carrying out finite element analysis for the tool pattern

This section involves the utilization of Finite Element Analysis to identify how the Cutting tool deforms during Machining. Finite Element Analysis enables the generation of accurate outcomes that aid scientists and engineers in comprehending the impact of various feed rates and cut depths on the cutting tool. This understanding can facilitate the optimization of the design process. I investigated the effect of the feed rate and the depth of the cut during machining. During this investigation, the Ansys software 2023 R1 has been used. The method used is an Explicit Dynamics.

The methods and procedures involved in this section are discussed in the following.

4.1 Engineering data

In this section, before starting my simulation, I defined the engineering materials of which the workpiece and the cutting tool are made. The workpiece used was made of structural steel and the cutting tool used was of High Speed Steel type. Their physical properties can be found in the tables below:

Engineering Data: Material View

High-Speed Steel	
Density	7.87e-06 kg/mm³
Structural	
Isotropic Elasticity	
Derive from	Young's Modulus and Poisson's Ratio
Young's Modulus	2.4e+05 MPa
Poisson's Ratio	0.3
Bulk Modulus	2e+05 MPa
Shear Modulus	92308 MPa

Table 3: Physical properties of High-Speed Steel[7]

4	Structural Steel			Fatigue Data at zero mean stress comes from 1998 ASME BPV Code, Section 8, Div 2, Table 5-110.1
*	Click here to add a new material			

Properties of Outline Row 4: Structural Steel

	A	B	C	D	E
1	Property	Value	Unit		
2	Material Field Variables	Table			
3	Density	7850	kg m^-3		
4	Isotropic Elasticity				
10	Specific Heat Constant Pressure, C_p	434	J kg^-1...		

Table 4: Physical properties of Structural steel

Structural Steel

Fatigue Data at zero mean stress comes from 1998 ASME BPV Code, Section 8, Div 2, Table 5-110.1

Density	7.85e-06 kg/mm³
Structural	
Isotropic Elasticity	
Derive from	Young's Modulus and Poisson's Ratio
Young's Modulus	2e+05 MPa
Poisson's Ratio	0.3
Bulk Modulus	1.6667e+05 MPa
Shear Modulus	76923 MPa
Isotropic Secant Coefficient of Thermal Expansion	1.2e-05 1/°C
Compressive Ultimate Strength	0 MPa
Compressive Yield Strength	250 MPa
Strain-Life Parameters	-6.6e-1

Figure 48: Material view of Structural steel

Structural steel is a versatile form of steel that is utilized as a building material in a variety of shapes. These shapes are frequently crafted with distinct cross-sectional profiles that resemble elongated beams.

Structural steel is engineered to have precise shapes and sizes that meet the requirements of various projects, such as buildings, highways, and bridges. Several techniques for manufacturing this specific material include hot milling, cold rolling, precision welding, and bending.

In addition, structural steel encompasses various types. Each is tailored for distinct purposes. Structural steel is available in a variety of shapes and grades, which are selected according to the specific requirements of the project. The categorization of structural steels is based on the configuration of their cross sections, with frequently employed profiles including I, T, and C forms. However, The grade of the steel has a direct impact on its mechanical qualities. Therefore, It is crucial to choose several grades of structural steel to fulfill different design requirements.[14]

4.2 Importing geometry

For this section, an assembled workpiece and the cutting tool have been imported. The file was a saved STEP file from the 3D model of the cutting tool and workpiece assembly. In this investigation, two models have been employed. The first one was created by varying the depth of cut and the second was created by varying the feed rate. Each model has been studied separately for proper results. The imported geometry is shown in the figure below.

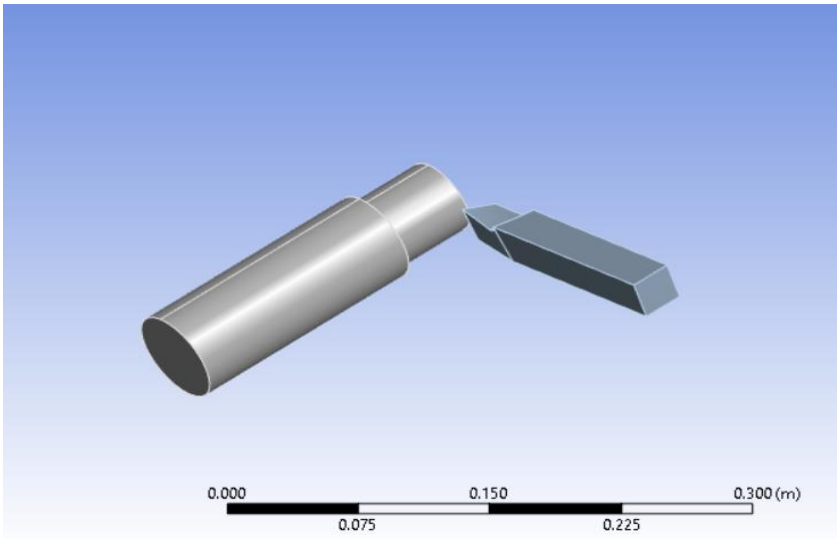

Figure 49: Geometry import of 3D model assembly for the study made while varying the depth of cut

4.3 Mesh set up

During the mesh setup, an element size of 0.2 was used. The element order was considered to be linear. I selected the linear type from quadratic due to the complex geometry of the cutting tool and it is best suited for faster solutions. The mesh refinement is very important because it enhances the quality of the results.

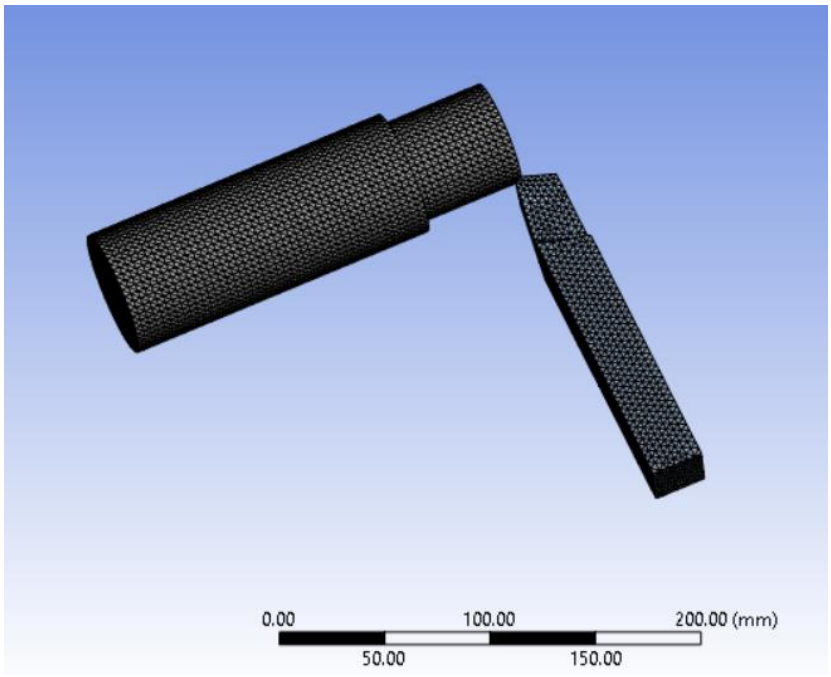

Figure 50: The mesh created on a 3D model for the study made while varying the depth of cut.

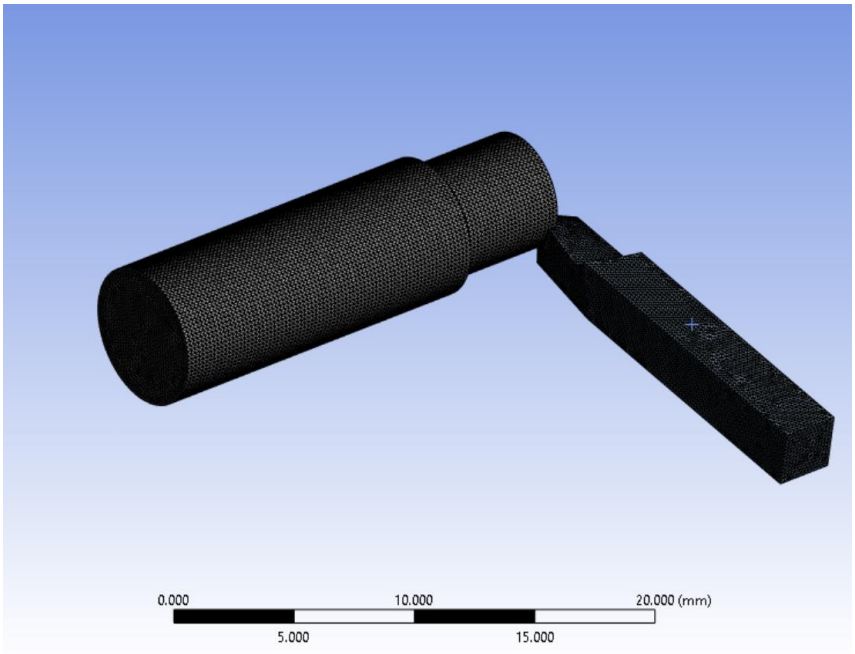

Figure 51: The mesh created on a 3D model for the study made while varying the feed rate.

4.4 Initial condition

4.5 By varying the depth of the cut

In this section, the initial condition parameters for Finite Element Analysis for the tool pattern were set. The workpiece was assigned an angular displacement in the coordinate axis and the cutting tool was defined under various depths of cut. The depths of cut used were 0.5 mm, 1 mm, 1.5mm, 2 mm, and 2.5 mm.

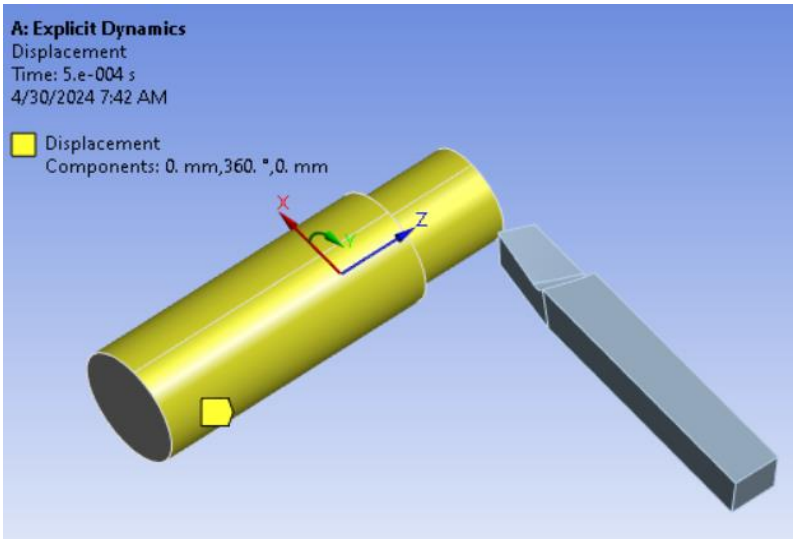

Figure 52: Displacement of the workpiece

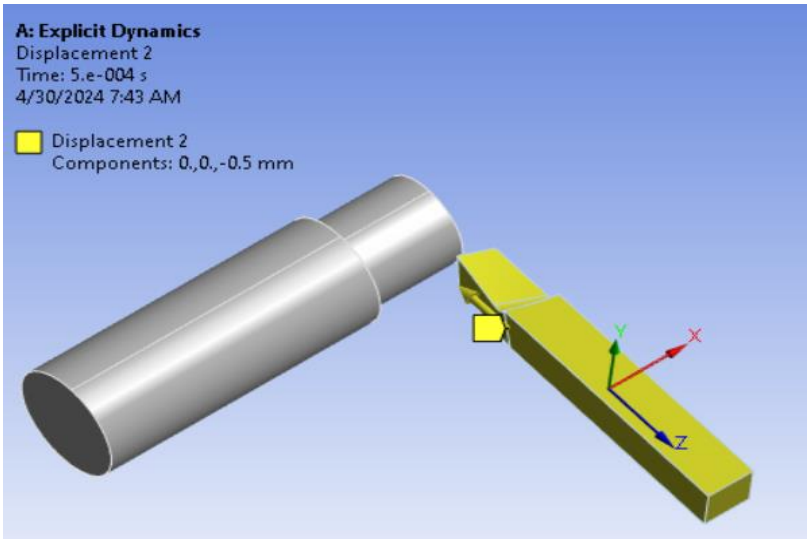

Figure 53: Displacement of the cutting tool

4.5.1 Contacts

The contact between the cutting tool and the workpiece was defined. The contact type has been defined as frictional. I defined the dynamic friction coefficient to be 0.4 and the frictin coefficient was taken 0.3 by interpolation.

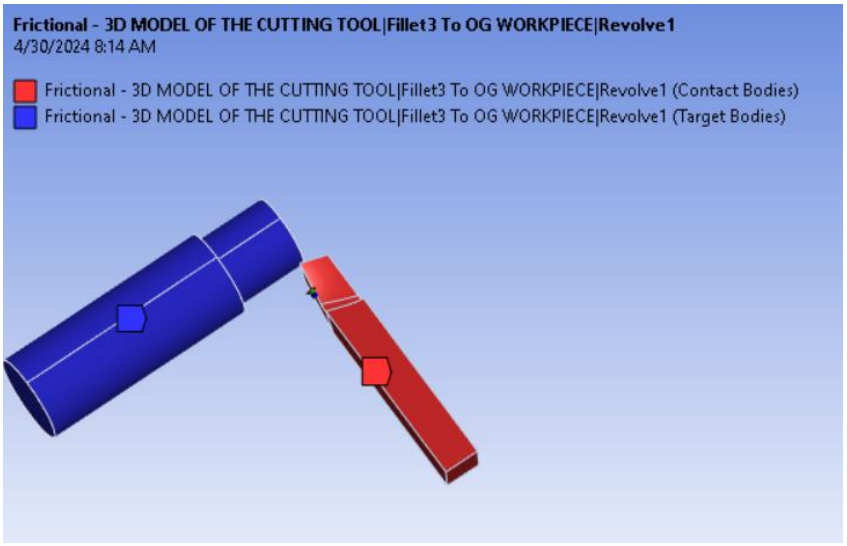

Figure 54: Defining the contact between the workpiece and the cutting tool

4.5.2 Run the simulation

A simulation was run after setting the initial condition. Different simulations were made with varying levels of cutting depth. The solution results consist of total deformation, the equivalent stress, and the reaction force for different depths of cut investigated.

4.5.3 Applying a depth of cut of 0.5 mm

Total deformation results

The results show that when a depth of cut of 0.5 mm is applied, a maximum deformation of 27 mm is experienced using the Finite Element Analysis. The distribution of the deformed areas is shown on the figure below.

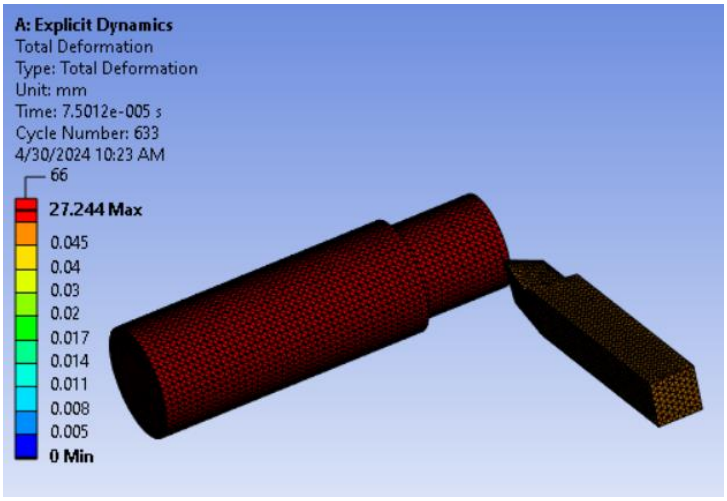

Figure 55: Total Deformation with a depth of cut of 0.5 mm.

Equivalent stress at a depth of cut of 0.5 mm

The figure below shows the results indicating the Equivalent (Von-Mises) stress distribution across the cutting tool and the workpiece. A maximum value of 16304 MPa was experienced as it can be shown in the figure below.

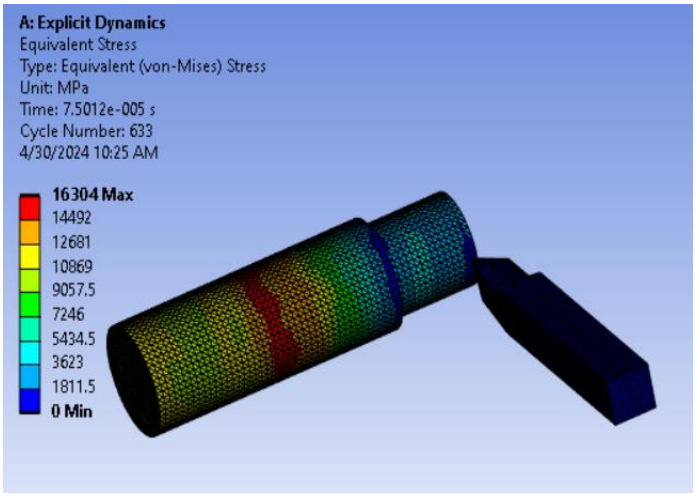

Figure 56: Equivalent stress with a depth of cut of 0.5 mm

Force Reaction

The figure below shows the resultant reaction force of 419.91 N.

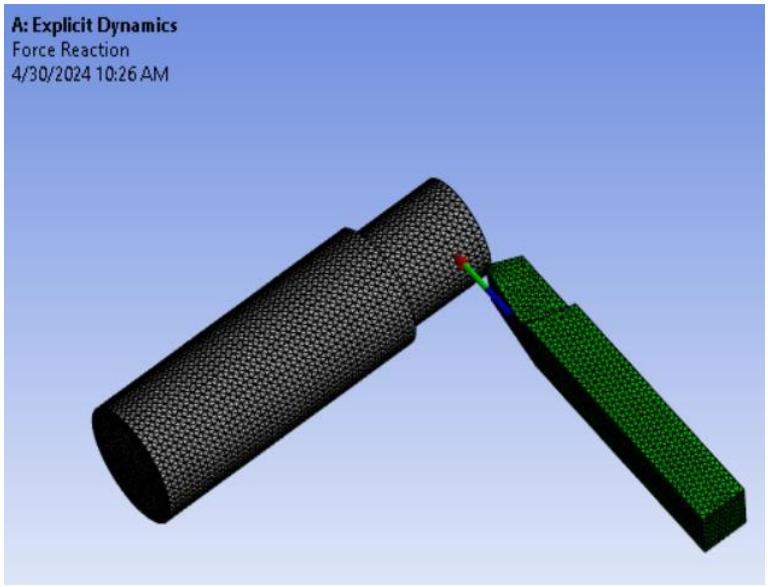

Figure 57: Force reaction with a depth of cut of 0.5 mm

A table of the results showing the maximum value over Time can be shown as follow:

Results	
Maximum Value Over Time	
X Axis	0. N
Y Axis	412.08 N
Z Axis	23.243 N
Total	419.91 N

Table 5: Maximum Value Over Time

4.5.4 Applying a depth of cut of 1 mm

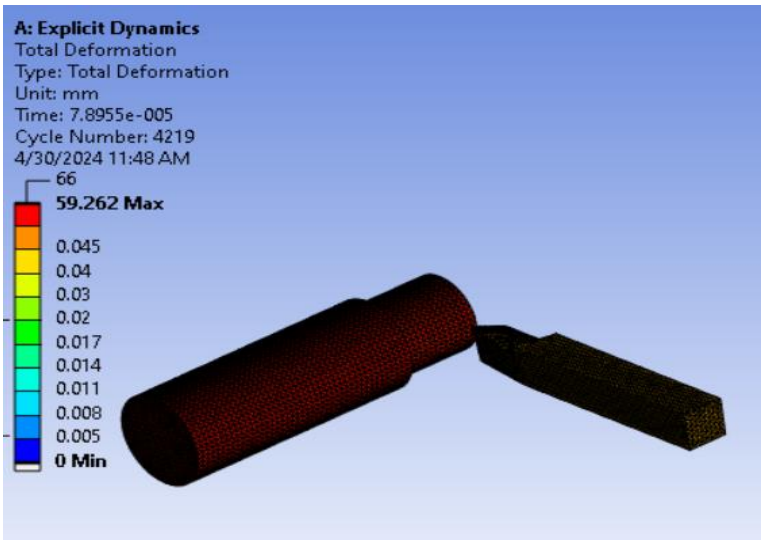

Figure 58: The total deformation in mm for a depth of cut of 1 mm

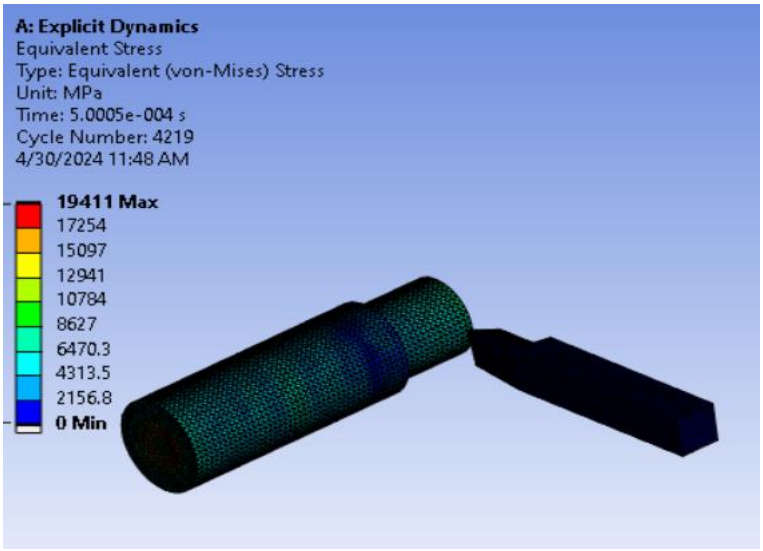

Figure 59: The equivalent (Von-Mises) stress for a depth of cut of 1 mm

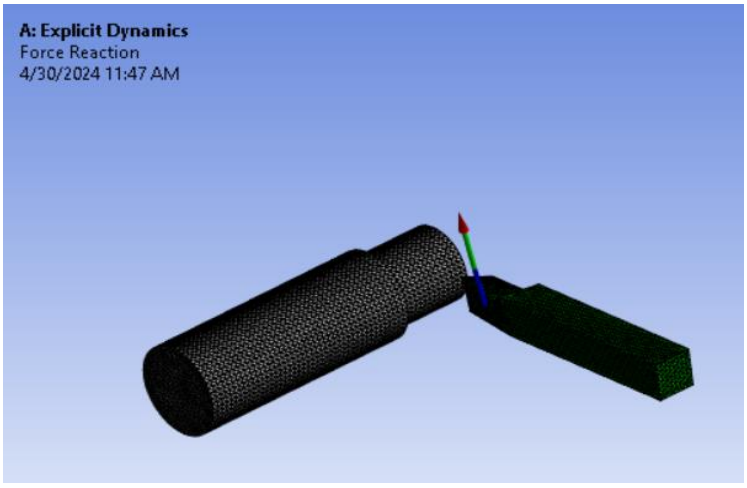

Figure 60: The force reaction with a depth of cut of 1 mm

A table of results showing Maximum Value over time can be shown in the following table:

Results	
Maximum Value Over Time	
X Axis	0. N
Y Axis	1531.6 N
Z Axis	197.33 N
Total	1563.8 N

Table 6: Reaction force of 1563.8 N for a depth of cut of 1mm

4.5.5 Applying a depth of cut of 1.5 mm

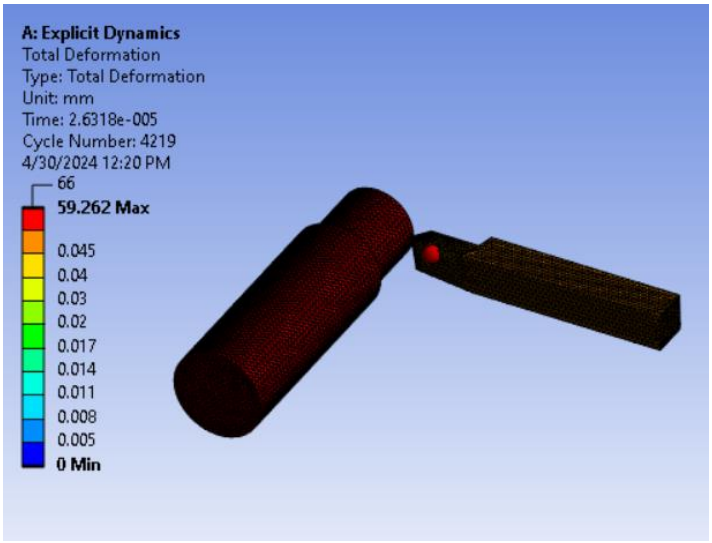

Figure 61: The Total deformation for a depth of cut of 1.5 mm

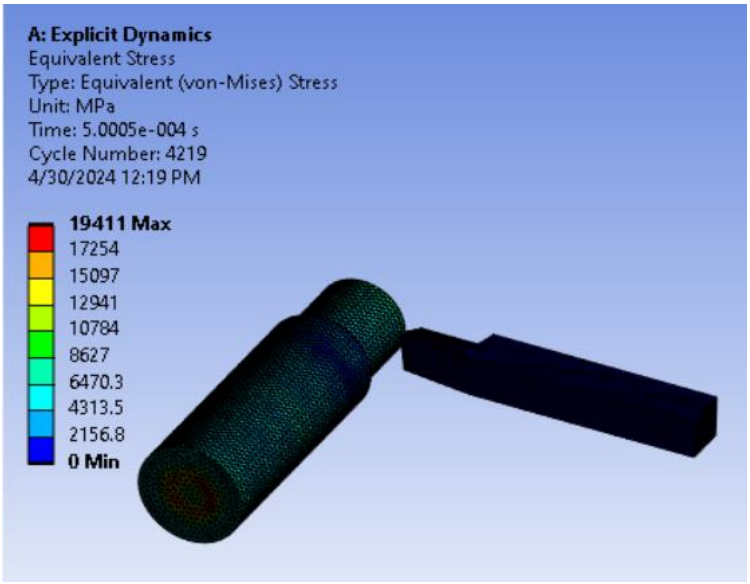

Figure 62: The Equivalent(Von-Mises) stress for a depth of cut of 1.5 mm

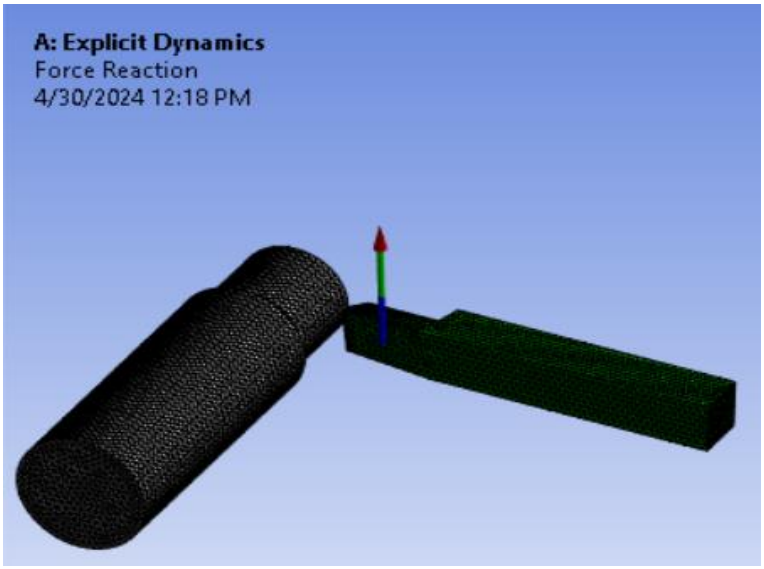

Figure 63: The force reaction of 2508.3 N for a depth of cut of 1.5 mm

4.5.6 Applying a depth of cut of 2 mm

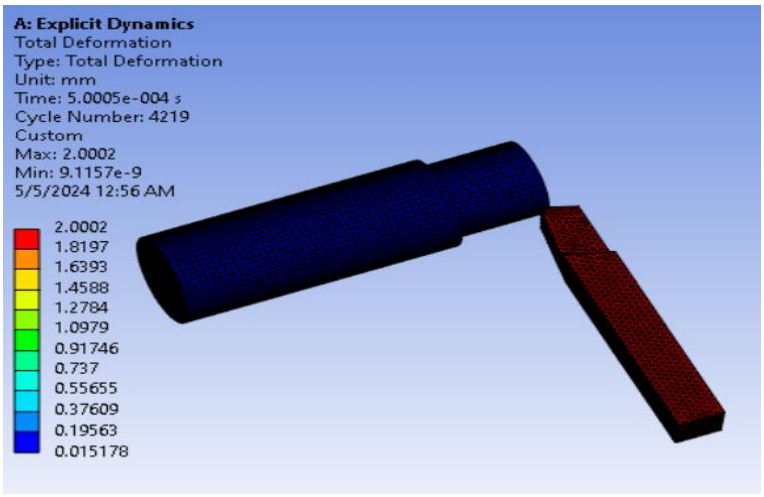

Figure 64: Total deformation with a depth of cut of 2 mm

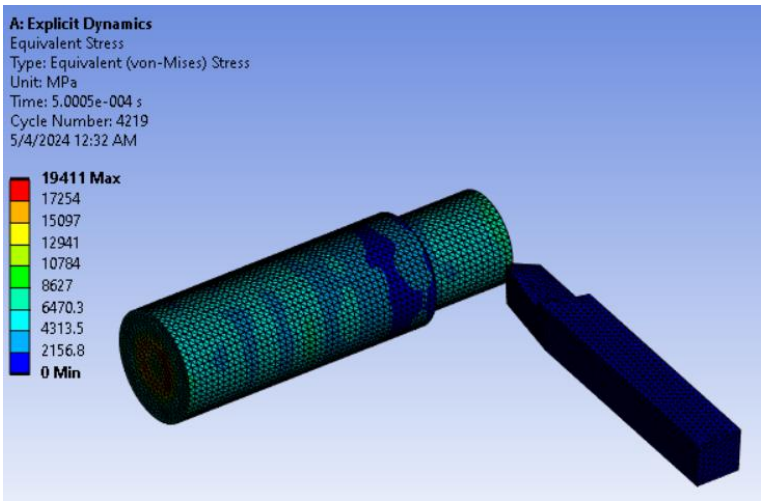

Figure 65: Equivalent stress with a depth of cut of 2 mm

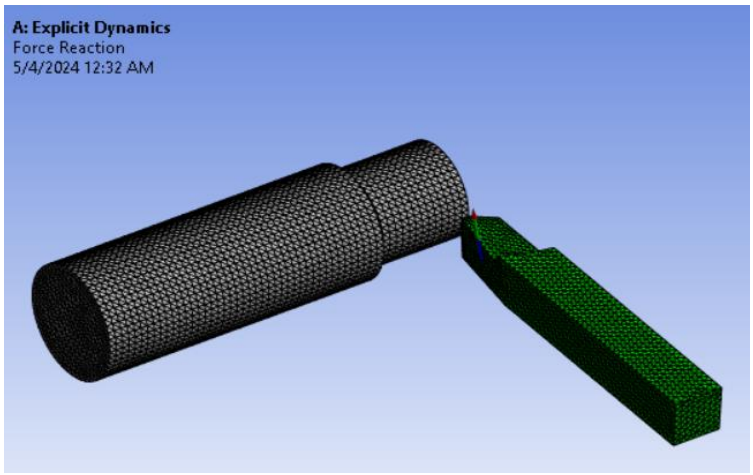

Figure 66: Reaction force with a depth of cut of 2 mm

Results	
Maximum Value Over Time	
X Axis	0. N
Y Axis	3914.4 N
Z Axis	174.1 N
Total	3970.9 N

Table 7: The reaction force of 3970.9 N developed at a depth of cut of 2mm

4.6 By Varying the feed rate

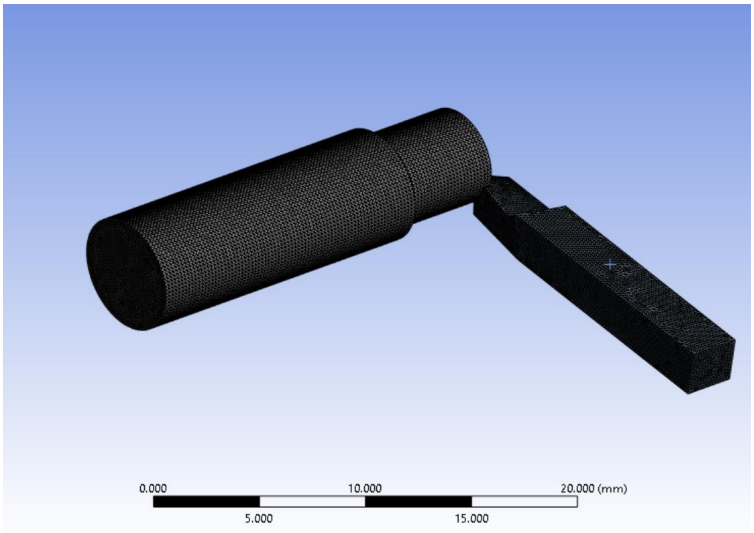

Figure Figure 67: A 3D model for feedrate analysis

4.6.1 Applying the feedrate of 0.1 mm/rev

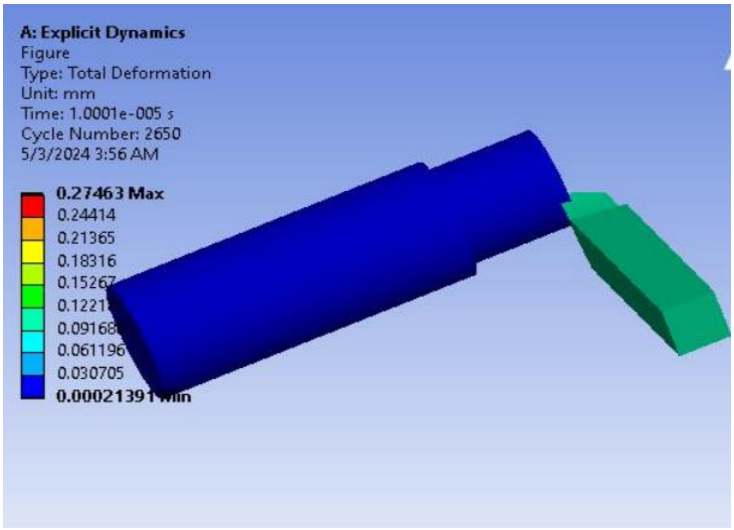

Figure Figure 68: Total deformation with a feedrate of 0.1 mm/rev

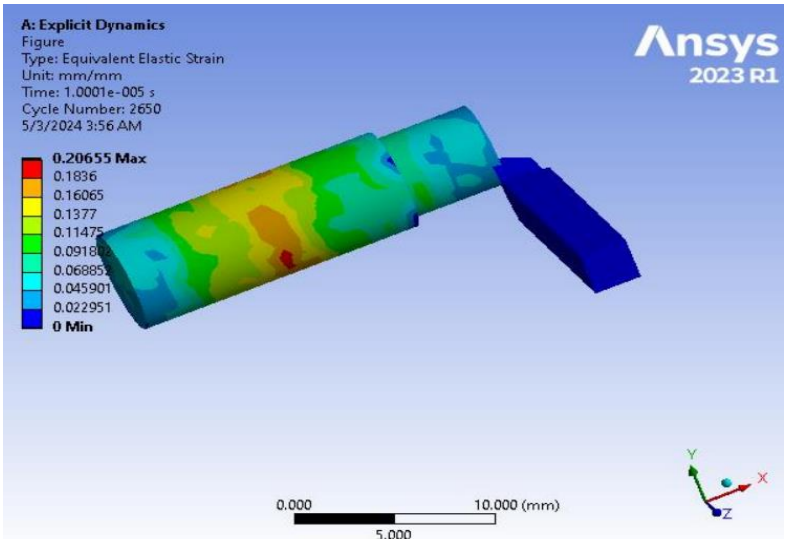

Figure 69: The equivalent Elastic strain with a feedrate of 0.1mm/rev

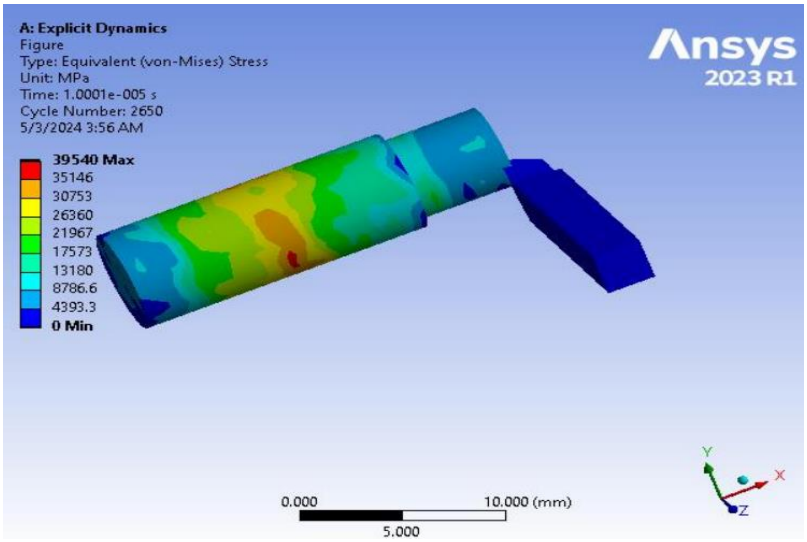

Figure 70: Equivalent stress with a feed rate of 0.1mm/rev

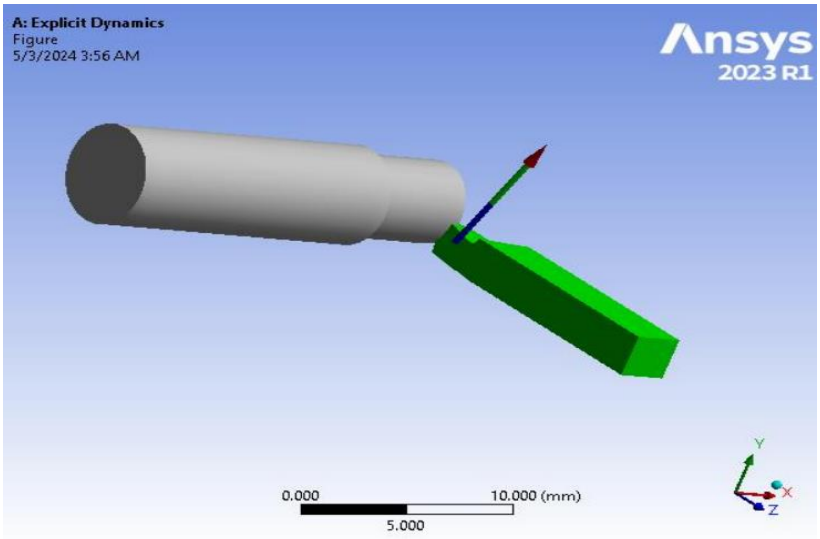

Figure71: The total Force with a feed rate of 0.1 mm/rev

Results	
Maximum Value Over Time	
X Axis	15285 N
Y Axis	1.0797e+005 N
Z Axis	38241 N
Total	1.1533e+005 N

Table 8: The resultant(reaction) force with a feed rate of 0.1mm/rev

4.6.2 Applying a feed rate of 0.2mm/rev

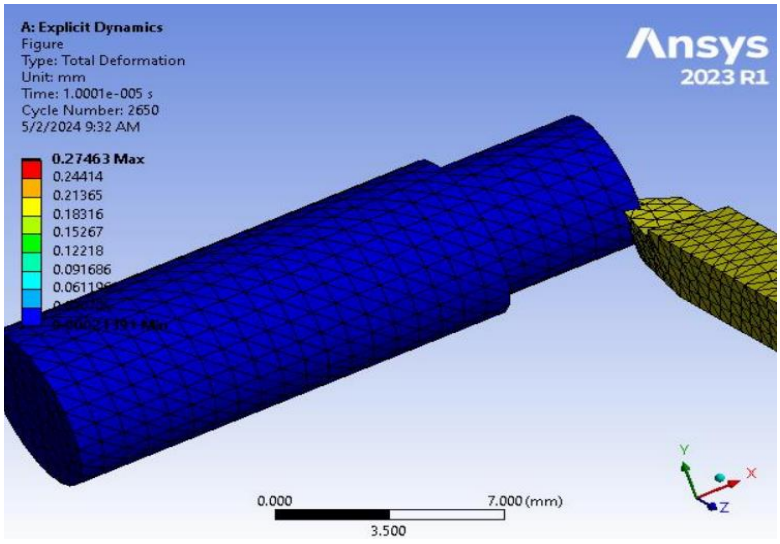

Figure 72: Total deformation with a feedrate of 0.2 mm

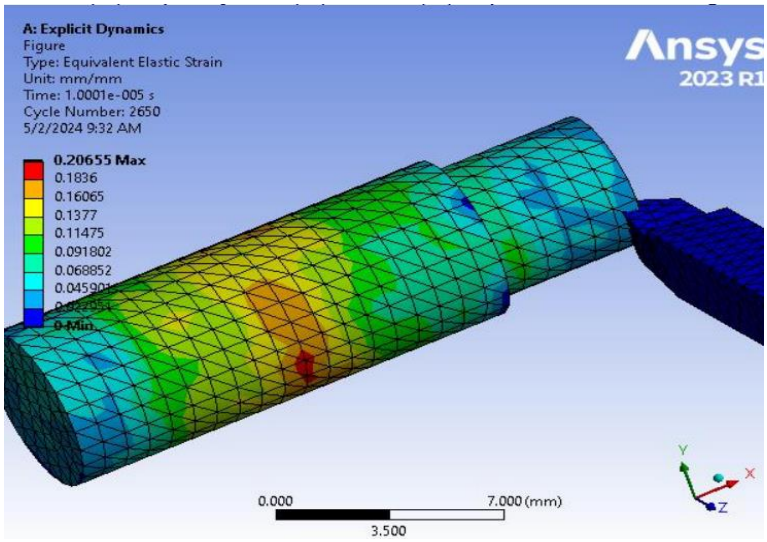

Figure 73: Equivalent Elastic strain with a feedrate of 0.2 mm

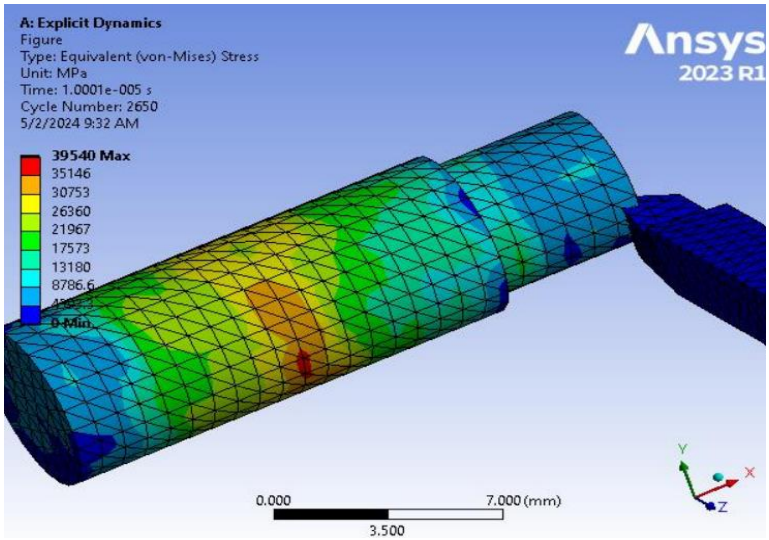

Figure 74: Equivalent (Von-Mises) stress with a feedrate of 0.2 mm

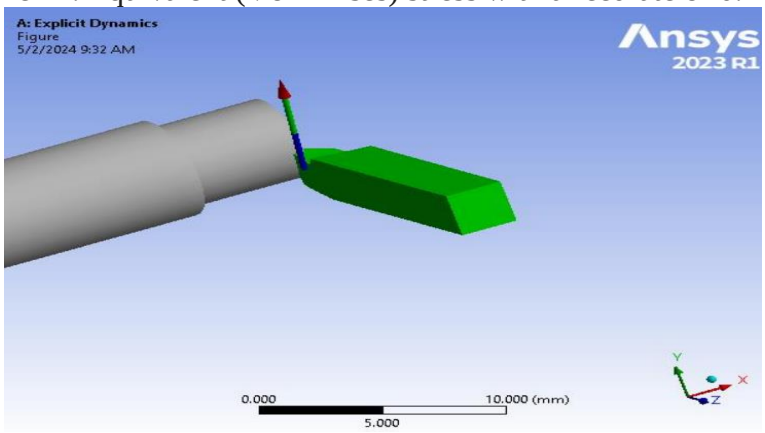

Figure 75: The reaction force with a feedrate of 0.2 mm/rev

Results	
Maximum Value Over Time	
X Axis	14303 N
Y Axis	1.1085e+005 N
Z Axis	38643 N
Total	1.1731e+005 N

Table 9: The reaction (resultant) force with a feedrate of 0.2 mm

4.6.3 Applying a feedrate of 0.3 mm/rev

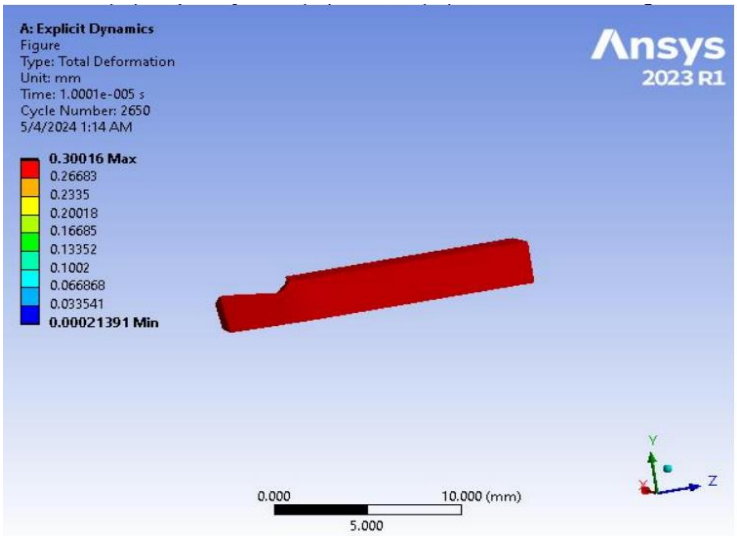

Figure 76: Total deformation with a feedrate of 0.3 mm

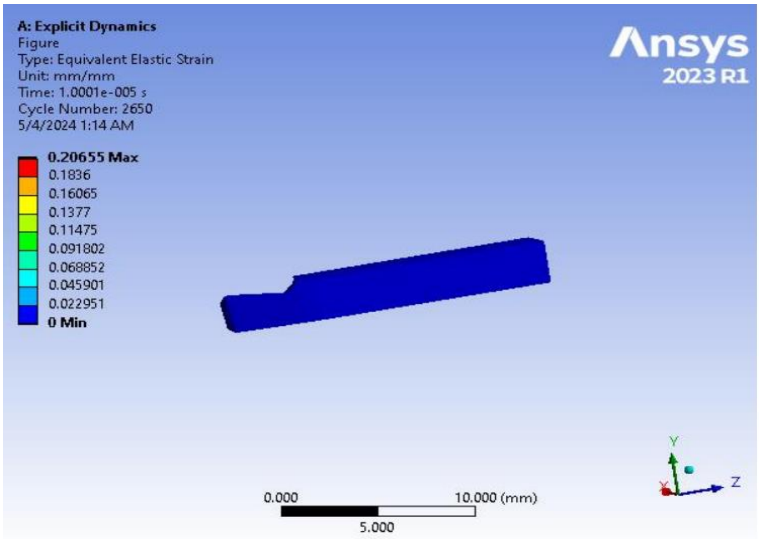

Figure 77: Equivalent Elastic strain with a feedrate of 0.3mm/rev

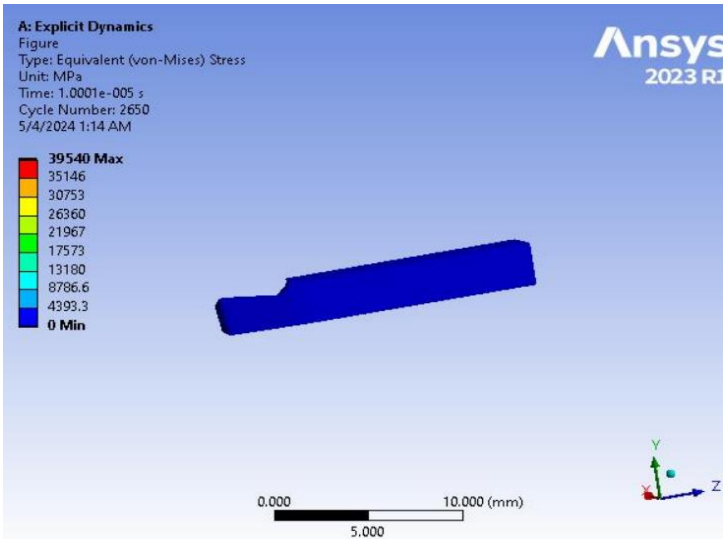

Figure 78: Equivalent (Von-Mises) stress with a feedrate of 0.3 mm/rev

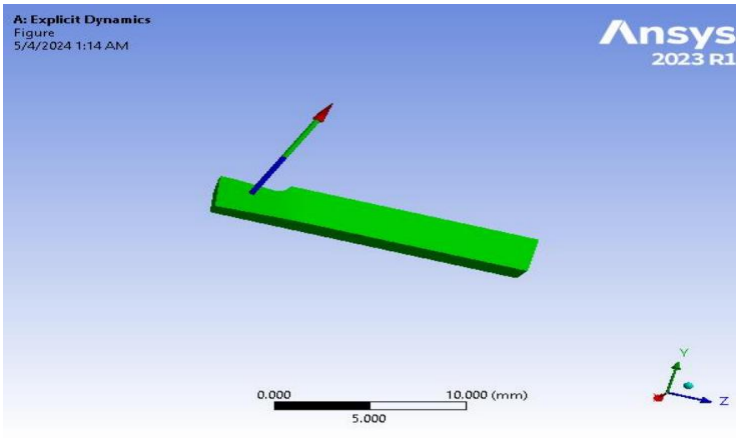

Figure 79: Total force with a feedrate of 0.3 mm/rev

Results	
Maximum Value Over Time	
X Axis	13319 N
Y Axis	1.0766e+005 N
Z Axis	37426 N
Total	1.1476e+005 N

Table 10: The reaction(resultant) force with a feedrate of 0.3 mm/rev

4.6.4 Applying a feedrate of 0.4 mm/rev

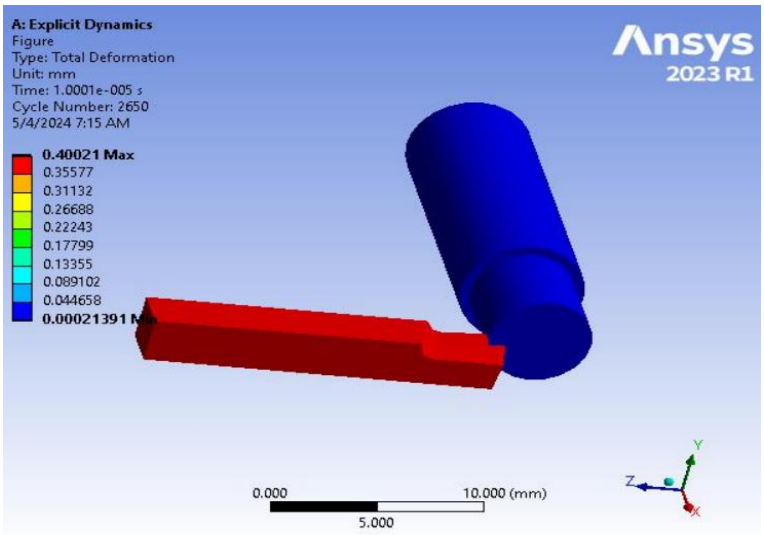

Figure 80: Total deformation with a feedrate of 0.4mm/rev

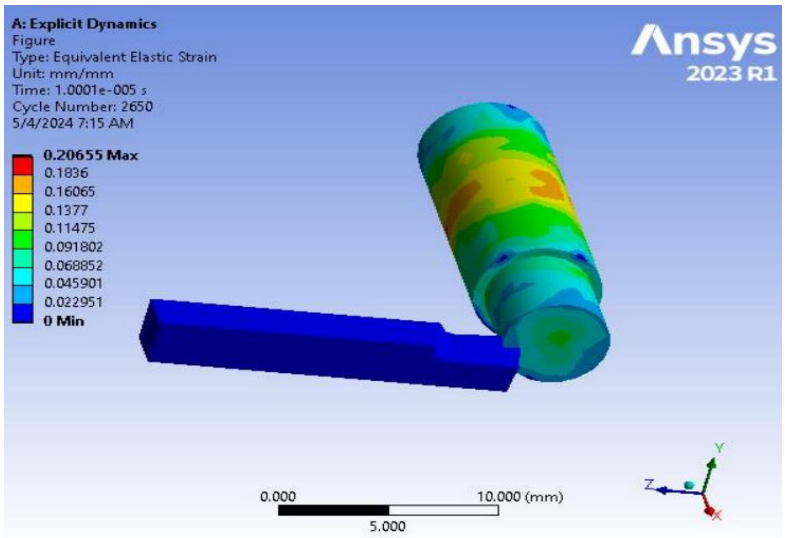

Figure 81: Equivalent Elastic strain with a feedrate of 0.4 mm/rev

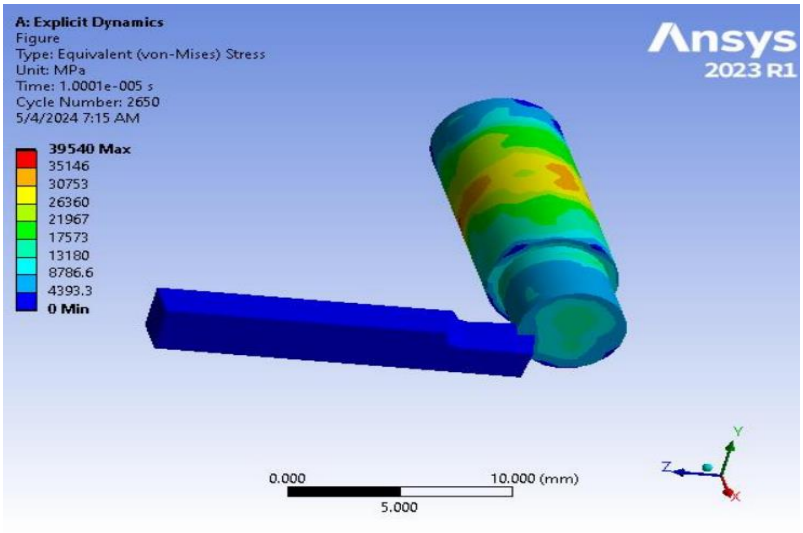

Figure 82: The equivalent(Von-Mises) stress

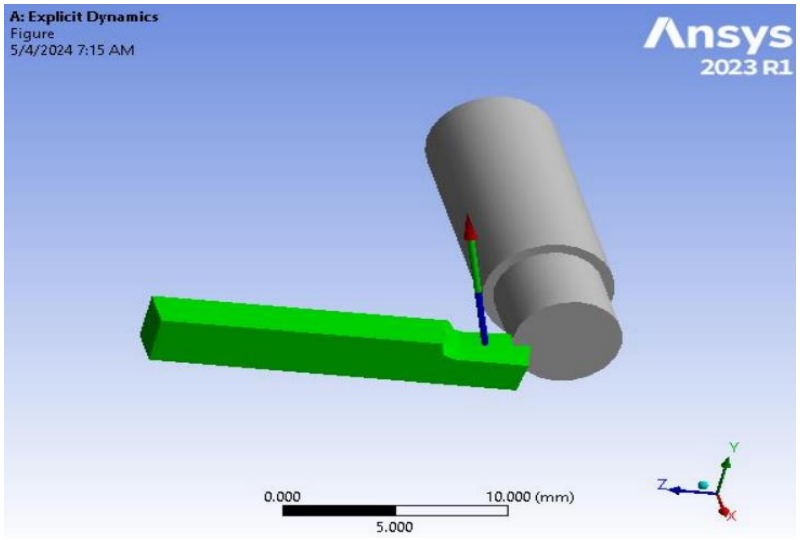

Figure 83: The total force with a feed of 0.4 mm/rev

Results	
Maximum Value Over Time	
X Axis	12338 N
Y Axis	1.0826e+005 N
Z Axis	37375 N
Total	1.151e+005 N

Table 11: The Maximum Over Time with a feed rate of 0.4mm/rev

5 Evaluation of the results and comparing with scientific research resources

This study examines the wear patterns of single-point cutting tools and explores methods for optimizing them. Once the 3D model of the cutting tool and the workpiece assembly were created, a Finite Element Analysis was conducted on the tool pattern. The resulting data was then combined and examined. I analyzed the total deformation, equivalent stress, and reaction force by utilizing a High-Speed Steel cutting tool and a structural workpiece material. This analysis involved varying the feed rates and depths of the cut. Initially, a graph illustrating the relationship between the Depth of cut and the total force has been generated. The findings indicate that there is a positive correlation between the depth of the cut and the overall force, meaning that as the depth of the cut grows, the total force also increases. I employed a range of depth of cut values, specifically 0.5, 1, 1.5, and 2 mm, together with feed rates of 0.1, 0.2, 0.3, and 0.4 mm/rev each revolution. The table below displays the results for the reaction forces.

.

Depth of cut	X (N)	Y (N)	Z (N)	Total Force (N)
0.5	0	412.08	23.243	**419.91**
1	0	1531.6	197.33	**1563.8**
1.5	0	2481.5	241.33	**2508.3**
2	0	3914.4	174.1	**3970.9**

Table 12: A summarized results obtained of various depths of cut (mm) and the corresponding reaction force.

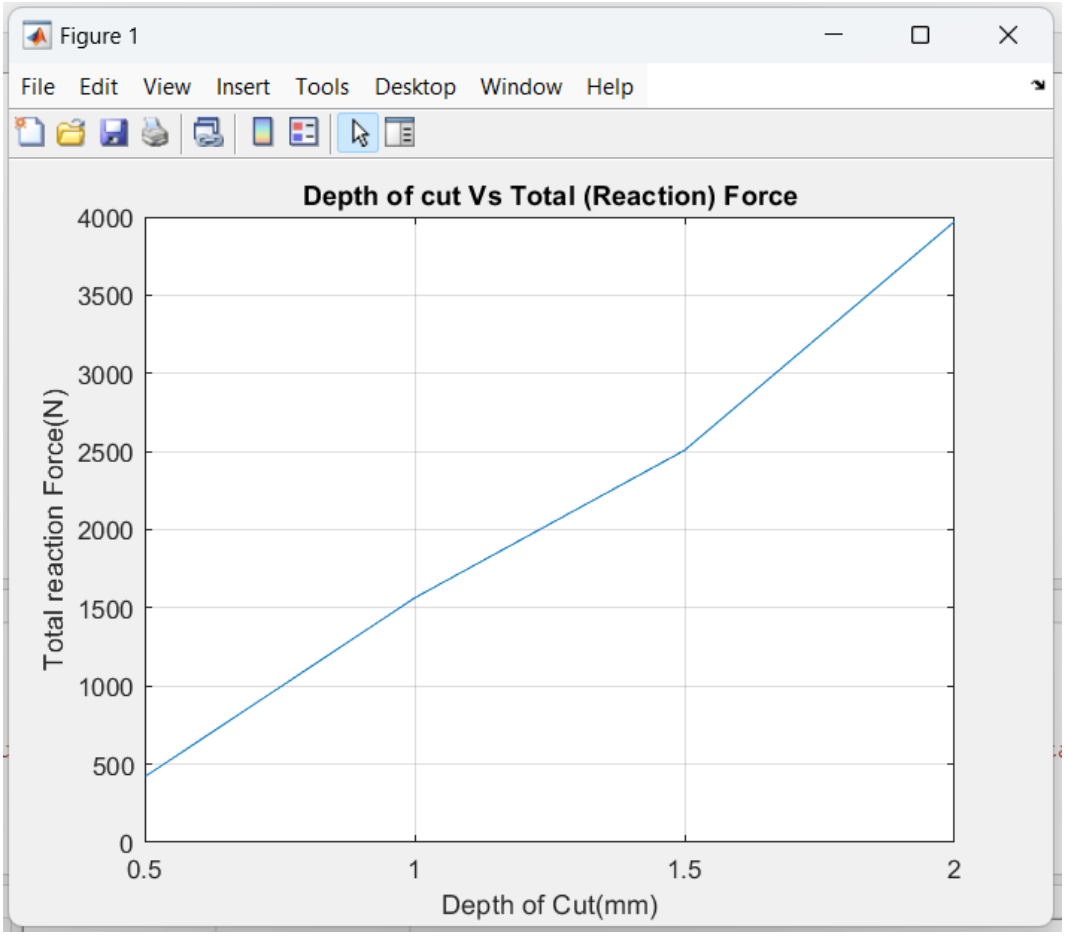

Figure 84: A graph of Depth of cut versus the total force

Feedrate results

	X (N)	Y (N)	Z (N)	Total Force (N)
0.1	15285	1.0797e+005	38241	**1.1533e+005**
0.2	14303	1.1085e+005	38643	**1.1731e+005**
0.3	13319	1.0766e+005	37426	**1.147e+005**
0.4	12338	1.0826e+005	37375	**1.151e+005**

Table 13: A summarized results of various feed rates (mm/rev) with the reaction forces generated

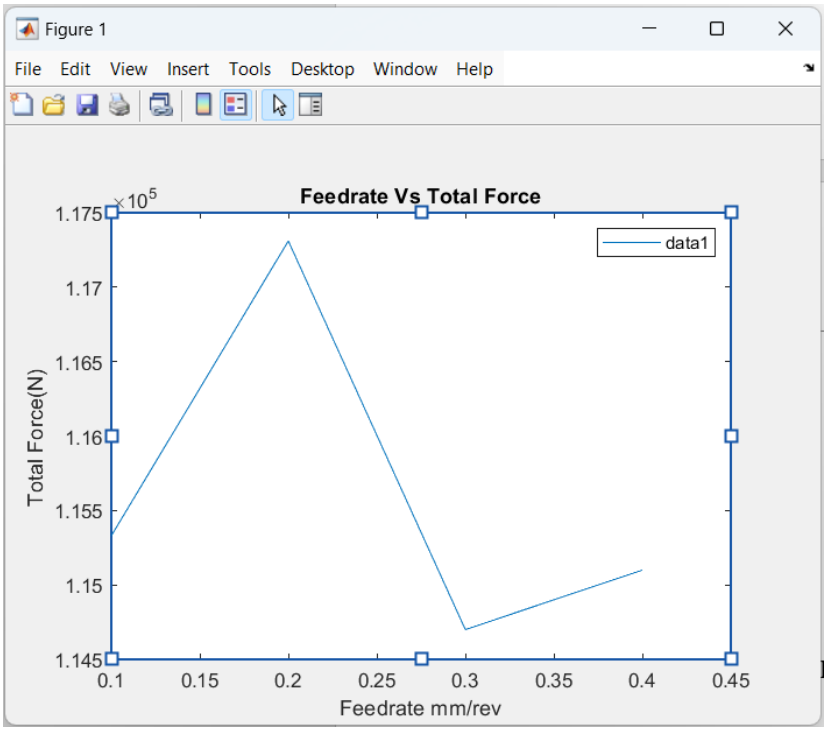

Figure 85: A graph of Feedrate vs Total Force

The results obtained from the Finite Element Analysis indicate that the smallest force necessary for the tool patterns occurs when a feed rate of 0.3 mm/rev is used. This demonstrates that a low force demand at a feed rate of 0.3mm/rev is more desirable.

6 Conclusion

The main objectives of this thesis consists of investigation of tool wear patterns and their optimization in single point cutting tool. Different research resources have been used to understand and figure out the wear zone, cause of the tool wearing and how we can optimize them. Proper suggestions and method to mitigate the tool wear have been investigated. Secondly, I used Solidworks software to create a 3D model of the cutting tool deformation during machining where I considered a turning process, It is with this fact I also modelled a cylindrical workpiece. I assembled the cutting tool and the workpiece in order to do further examination.

To analyse the tool wear patterns, I used Ansys software Explicity dynamics because I wanted to see how the tool behaves under various cutting parameters such as feed rate and depth of cut. Firstly, I used different depths of cuts and obtained the results for total deformation, Equivalent(Von-Mises) stress, Equivalent Elastic Strain and the reaction force. An increase in the depth of cut resulted with an increase with the cutting force, elastic strain and eqivalent (Von-Mises) stresses. This relationship aligns with the scientific research resources as I previously discussed it in the literature review.

Secondly, I fixed the depth of cut and varied the feed rate. After applying different values of the depth of cut, I noticed a change, the increase of the cutting force was independent of an increase in the depth of cut. At some feed rate, the cutting force was increasing while at the others it was decreasing. I found that at certain values of feedrate and depth of cut, the tool would perform better with less or no deformation.

All in all, the scientific research resources showed that the tool wear patterns can be influenced by the cutting conditions such as dry or such as the feedrate, the depth of cut, the cutting tool material and the material of the workpiece.

7 List of references / Bibliography

[1] S. Sundaram, P. Senthilkumar, a Kumaravel, and N. Manoharan, "Study of Flank Wear in Single Point Cutting Tool Using," *Network*, vol. 3, no. 4, pp. 32–36, 2008.

[2] B. Kareem and M. O. Idris, "Modeling flank wear hardness of selected HSS and HCS single point cutting tools with or without cutting fluid," *Adv. Mater. Res.*, vol. 367, pp. 273–277, 2012, doi: 10.4028/www.scientific.net/AMR.367.273.

[3] M. Soori and B. Arezoo, "Cutting Tool Wear Prediction in Machining Operations, A Review." [Online]. Available: https://www.researchgate.net/publication/364283734

[4] "Tool Wear and Tool Life."

[5] T. Analysis, O. Single, P. Cutting, T. Using, and D. Cutting, "International Journal of Informative & Futuristic Research ISSN : 2347-1697 Thermal Analysis Of Single Point Cutting Tool Using Different Cutting Conditions," vol. 3, no. 9, pp. 3472–3483, 2016.

[6] M. Bourdim, L. Zouambi, M. D. Beida, and S. Kerrouz, "Determination of a Wear Law for Uncoated Cutting Tools," *Int. J. Syst. Appl. Eng. Dev.*, vol. 16, pp. 60–65, May 2022, doi: 10.46300/91015.2022.16.12.

[7] M. K. Srinath, M. S. G. Prasad, and R. Nazareth, "Static & dynamic performance analysis and modal simulations of single point cutting tool," in *IOP Conference Series: Materials Science and Engineering*, Institute of Physics Publishing, Jun. 2020. doi: 10.1088/1757-899X/872/1/012073.

[8] R. Rana, R. Lal, K. Rajput, and R. Saini, "Optimization of Tool Wear: A Review," 2014. [Online]. Available: https://www.researchgate.net/publication/280609317

[9] Y. Dogu, E. Aslan, and N. Camuscu, "A numerical model to determine temperature distribution in orthogonal metal cutting," *J. Mater. Process. Technol.*, vol. 171, no. 1, pp. 1–9, 2006, doi: 10.1016/j.jmatprotec.2005.05.019.

[10] L. Notes and C. Das, "Objective : To remove greatest amount of material in the shortest length of time Lecture Notes of Chinmay Das," pp. 1–13.

[11] M. Al Huda, "An Effect of Oil-Mist on Tool Wear in Turning," *Proc. Conf. Hokuriku-Shinetsu Branch*, vol. 2002.39, no. 0, pp. 37–38, 2002, doi: 10.1299/jsmehs.2002.39.37.

[12] J. A. Olortegui-Yume and P. Y. Kwon, "Tool wear mechanisms in machining," *Int. J. Mach. Mach. Mater.*, vol. 2, no. 3–4, pp. 316–334, 2007,

doi: 10.1504/ijmmm.2007.015469.

[13] S. Shaojun, Z. Xianping, and S. Chengtong, “Heat-treatment and properties of high-speed steel cutting tools,” *IOP Conf. Ser. Mater. Sci. Eng.*, vol. 423, no. 1, 2018, doi: 10.1088/1757-899X/423/1/012031.

[14] A. Fatima, M. Wasif, A. Ahmed, and S. Yaqoob, “Effect of rake face surface of cutting tool on tool crater wear,” *Manuf. Rev.*, vol. 10, p. 15, Oct. 2023, doi: 10.1051/mfreview/2023013.

[15] V. C. Venkatesh, S. Izman, T. C. Yap, N. S. M. El-Tayeb, and P. V Brevern, “Cryogenic Facing of Ti6Al-4V Alloys,” *Proceeding of ICOMAST*, no. August 2019, 2006.

[16] “Fundamentals_of_Modern_Manufacturing_Mikell_P_Groover 2.pdf.”

[17] A. Nuzulia, *Manufacturing processes Second ed page 313*. 1967.

[18] T. Parhizkar, T. Stewart, L. Huang, and A. Mosleh, “Degradation and Failure Mechanisms of Complex Systems: Principles,” *Ind. Appl. Math.*, vol. Part F2111, pp. 1–50, 2023, doi: 10.1007/978-981-19-9909-3_1.